UNIVERSITY OF TARTU

FACULTY OF SCIENCE AND TECHNOLOGY

INSTITUTE OF MOLECULAR AND CELL BIOLOGY

BIOTATEC OÜ

Bioleaching of phosphorus and rare earth elements (REEs) from Estonian phosphorite using *Aspergillus japonicus*

Bachelor's thesis

12 ECTS

Keity-Carol Topper

Supervisors

BSc Gintare Liudžiute

PhD Priit Jõers

TARTU 2025

Bioleaching of phosphorus and rare earth elements (REEs) from Estonian phosphorite using *Aspergillus japonicus*

Abstract. Phosphorite is conventionally solubilized through chemical processes, which results in high costs and environmental pollution. The phosphate rock mined to produce phosphorus is a finite resource, which makes production and supply vulnerable to risk. Around 1,1 million tonnes of phosphorus fertilizer is used in the EU yearly. As an environmentally friendlier and more cost-effective alternative, bioleaching by *Aspergillus japonicus* was studied for its potential to solubilize phosphorus and REEs. Results show that *A. japonicus* could effectively solubilize phosphorus in NBRIP medium, while REEs remain insolubilized in batch experiments. However, some REEs (Y, La, Ce, Nd) are leached in the semi-continuous culture.

Keywords: Bioleaching, *Aspergillus japonicus*, phosphorite

CERCS: B230 Microbiology, bacteriology, virology, mycology; T440 Non-metallic mineral technology; T490 Biotechnology; T360 Biochemical technology

Fosfori ja haruldaste muldmetallide (REEde) bioleostamine Eesti fosforiidist *Aspergillus japonicus*'ega

Lühikokkuvõte. Fosforiiti lahustatakse tavapäraselt keemiliste meetoditega, mille tagajärjeks on suured kulud ja keskkonnareostus. Fosfori tootmiseks kaevandatav fosfaatkivim on piiratud ressurss, mis muudab fosfori tootmise ja tarnimise riskide suhtes haavatavaks. EL-is kasutatakse aastas umbes 1,1 miljonit tonni fosforväetist. Keskkonnasõbralikuma ja kulutõhusama alternatiivina uuriti *Aspergillus japonicus*e potentsiaali bioleostada fosforit ja REEsid fosforiidist. Tulemused näitavad, et *A. japonicus* võib fosforit NBRIP söötmes tõhusalt lahustada, kuid perioodilises eksperimendis püsivad REEd lahustumatul kujul. Siiski, mõned REEd (Y, La, Ce, Nd) leostusid poolpidevkultuuris.

Märksõnad: Bioleostamine, *Aspergillus japonicus*, fosforiit

CERCS: B230 Mikrobioloogia, bakterioloogia, viroloogia, mükoloogia; T440 Mittemetalliliste mineraalide tehnoloogia; T490 Biotehnoloogia; T360 Biokeemiatehnoloogia

TABLE OF CONTENTS

TABLE OF CONTENTS 3

TERMS, ABBREVIATIONS AND NOTATIONS 5

INTRODUCTION 6

1. LITERATURE REVIEW 8

1.1. Estonian phosphorite 8

1.2. Bioleaching and organisms 9

1.2.1. Redoxolysis 12

1.2.2. Acidolysis 13

1.2.3. Complexolysis 16

1.2.4. Bioleaching of phosphate rocks by filamentous fungi 17

1.2.4.1. The media used for PSF cultivation 20

1.2.4.2. *Aspergillus japonicus* 22

1.3. Industrial bioleaching solutions 22

1.3.1. Stirred reactors 23

1.3.2. Stacked column 23

1.3.3. Heap bioleaching 24

2. EXPERIMENTAL PART 27

2.1. The aims of the thesis 27

2.2. Materials and methods 27

2.2.1. Substrate enrichment 27

2.2.1.1. Acid digestion of concentrated fraction 28

2.2.2. *A. japonicus* growth conditions 28

2.2.3. Bioleaching experiments 29

2.2.3.1. Determination of phosphorus content 31

2.2.3.2. Determination of metal content 31

2.2.3.3. Measurement of organic acid production 32

2.2.4. Statistical analysis....32
2.3. Results and discussion....32
2.3.1. Phosphorite composition....32
2.3.2. Sample collection test....34
2.3.3. Initial bioleaching experiment....35
2.3.4. Leaching using different C/N ratios with NBRIP in batch culture....36
2.3.5. Leaching using C/N=200 NBRIP in semi-continuous setup....40
2.3.6. Leaching using C/N=50 NBRIP semi-continuous setup....43
2.3.7. Organic acid measurements using assay kits....45
2.3.8. Future prospects....47
SUMMARY....48
RESÜMEE....49
REFERENCES....51
WEBPAGES....57
APPENDICES....58
APPENDIX 1. P-values....58
APPENDIX 2. Phosphorus solubilization by blanks....60
APPENDIX 3. The initial experiment on day 14....61
APPENDIX 4. Problems with organic acid measurements....62
Non-exclusive licence to reproduce the thesis and make the thesis public....65

TERMS, ABBREVIATIONS AND NOTATIONS

A. japonicus – *Aspergillus japonicus*

ICP-MS – inductively coupled plasma mass spectrometry

ppm – parts per million

PSF – phosphate-solubilizing fungi

PSI – phosphate solubilizing index

REE – rare earth element

RP – rock phosphate

rpm – revolutions per minute

INTRODUCTION

Phosphorus is essential for plant growth, making it a critical resource in agricultural fertilizers, thus supporting global food production. Phosphorus is produced by mining phosphate rock, which is a finite resource, and its production and supply are vulnerable to geopolitical risk. From 2012 to 2021 around 1,1 million tonnes of phosphorus fertilizer was used yearly in the European Union (European Commission, 2024). One of the biggest phosphate fertilizer producers in the world are Russia and Belarus (European Commission, 2024). According to the European Commission, the war between Russia and Ukraine led to higher fertilizer prices, which reduced the consumption rate of phosphate fertilizer in 2022 by 17,9% compared to 2021.

Rare earth elements (REEs) are important components in various high-tech devices, such as electric cars, wind turbines, solar panels, fluorescent and LED light bulbs, but also in military technology like communication equipment, radar technology and missile guidance systems. The supply of REEs is heavily concentrated in China, due to there being large reserves and aggressive governmental policy to control resources. Phosphorite production in the world is around 250 million tons per year and phosphate rock generally contains about 0,05 wt% of REEs, which makes it a considerable resource for REEs (S. Wu *et al.*, 2018). Estonia has unmined phosphorite reserves that contain 4-20% phosphorus in the form of P_2O_5. Additionally, Estonian phosphorite contains some REEs (Y, La, Ce, Nd, Sm, Pr and Gd), with the total REE concentration of 1026±23 ppm (=mg/kg), from which around 90% are light REEs (La, Ce, Pr and Nd) (Suomalainen, 2024). Both resources (phosphorus and REEs) are strategically important and securing sustainable and local sources in Europe is crucial for economic stability and environmental resilience.

Phosphorite is conventionally processed by chemical leaching using sulfuric acid (H_2SO_4), which can produce hazardous waste. Other acids for chemical leaching include nitric acid (HNO_3) for both phosphorus and REE extraction and hydrochloric acid (HCl) for REE extraction. The process of chemical leaching with sulfuric acid produces large quantities of phosphogypsum, which contains radioactive and toxic elements such as uranium, thorium, and cadmium (Shi *et al.*, 2024). The phosphogypsum is usually stored in open stacks, posing a risk of leaching said elements into groundwater. Other byproducts of chemical leaching include acidic and fluoride-rich wastewater, as well as volatile pollutants like HF gas. In contrast, bioleaching is more environmentally friendly and energy-efficient than traditional REE

extraction methods. This method is conducted at near room temperature and generates significantly lower CO_2 emissions. Bioleaching does not require harsh chemicals, unlike chemical leaching, and does not emit toxic gases. This can make bioleaching a cost-effective alternative, allowing economically feasible processing of even low-grade ores.

The literary part of this work provides an overview of phosphorite, bioleaching mechanisms, industrial bioleaching solutions and the usage of phosphate-solubilizing fungi (PSF) in rock phosphate leaching. The work focuses on *Aspergillus japonicus*, that is one of the most commonly used fungi in phosphate solubilization. In the experimental part of this work, phosphorite processing, cultivation of *A. japonicus*, media optimization, bioleaching experiments and analysis of phosphorus, metal and acid content are described.

The thesis aims to study the bioleaching potential of phosphorite with *A. japonicus* to extract phosphorus and REEs. The work was done at BiotaTec OÜ.

1. LITERATURE REVIEW

1.1. Estonian phosphorite

Phosphorite, rock phosphate (RP) or phosphatic rock is a rock that contains high amounts of phosphate minerals, which are minerals that contain a tetrahedrally coordinated phosphate anion (PO_4^{3-}) (Mackey & Paytan, 2009). Phosphorite typically contains 15%-20% phosphorus pentoxide (P_2O_5), which is mostly present as fluorapatite and hydroxyapatite. The theoretical maximum amount of P_2O_5 in pure fluorapatite ($Ca_5(PO_4)_3F$), calculated by molecular weight, is approximately 422 mg/g (42,4%). Estonia possesses some of Europe's largest phosphorite reserves, estimated by Tiit Kaasik, the head of the Department for Geological Resources at the Geological Survey of Estonia, at approximately 2.9 billion tons (Saluorg, 2023). Estonian phosphorite reserves are located in Rakvere, Toolse, Aseri, Tsitre and Maardu (Raukas & Teedumäe, 1997). The investigation into Estonian phosphorite began as early as 1920, following shortages of phosphate fertilizers after World War I. The first mine began operating in 1924 at Ülgase and the second one in 1940 at Maardu. The Soviet Union had ambitious plans, in the 1970s-1980s, for large-scale mining of Estonian phosphorite, to secure a domestic source of phosphate fertilizer. There was great opposition to the mining of phosphorite in Estonia due to the threat of environmental pollution. Namely, at the end of the 1980s, there was a wave of protests, called the Phosphorite War (fosforiidisõda). Currently, no phosphorite is being mined in Estonia, although test drilling began in 2024 at Lääne-Virumaa to determine the value of the phosphorite (Kundla, 2024).

Estonian phosphorite is rich in shell debris, containing remnants of brachiopods from as early as the late Cambrian and early Ordovician periods, during which the Baltica plate was situated in the southern hemisphere of the globe (Cocks & Torsvik, 2005; Raukas & Teedumäe, 1997). Estonian phosphorites P_2O_5 is in a range of 6-20%, while the brachiopod shells and detritus contain up to 35-37% P_2O_5 (Raukas & Teedumäe, 1997). Phosphate ores' P_2O_5 content of below 16% is considered low grade, 17-25% medium and 26-35% high grade phosphorite (Sengul *et al.*, 2006). The biogenic fraction, brachiopod shells and detritus, of Estonian phosphorite is therefore high-quality material for phosphate extraction.

Estonian phosphorite also contains several other elements, REEs and uranium (U) among them, which typically occur in the brachiopod detritus. REEs mostly substitute Ca^{2+} ions in the apatite commonly occurring in phosphorite (Graul *et al.*, 2023). A recent study used

phosphorite samples from Toolse and found the average REE concentrations to be 805 ± 108 ppm (Maardu), 431 ± 125 ppm (Suurjõgi) or 151 ± 75 ppm (Katela) based on the allocated category according to the stratigraphy of the Kallavere Formation (Graul *et al.*, 2023). The most frequently occurring REEs in those samples were Ce, Y, Nd, and La. The U concentrations in Estonian phosphorite deposits are relatively low at 24 ± 6 ppm and 15 ± 4 ppm in the Toolse and Rakvere deposits, respectively; overall, only few locations in Rakvere have U concentrations exceeding 25 ppm (Soesoo *et al.*, 2020).

1.2. Bioleaching and organisms

Bioleaching is a metal extraction method that utilizes microorganisms, such as bacteria and fungi, but also archaea, algae and yeasts. This method is based on the ability of microbes to interact with the metal-containing compounds or their environment in a way that releases the metals into solution. Historically, bioleaching has been especially important for extracting metals from copper deposits.

Throughout bioleaching history, the most commonly used microorganisms have been chemoautotrophic bacteria. Chemoautotrophs oxidize inorganic substances (such as iron and sulfur compounds) to obtain energy, and they use CO_2 fixation to obtain carbon. These organisms create an acidic environment and produce strong oxidizing agents (such as Fe^{3+} and H^+) that decompose metal sulfides (such as chalcopyrite – $CuFeS_2$), releasing metals such as copper (Cu) and gold (Au).

Commercial bioleaching of copper began in the 1950s in Bingham Canyon Mine, USA (Copper Development Association, 2004). A major developer in copper bioleaching on an industrial scale is Chile, where 30% of the world's copper is produced, from which 10% is produced using bioleaching (Tanaka, 2017). Chalcopyrite ($CuFeS_2$) is the most common copper mineral, it can be oxidized using chemoautotrophic bacteria *Thiobacillus ferrooxidans* and *Thiobacillus thiooxidans* (Copper Development Association, 2004). At present, the extraction of copper from low-grade ores is being done using bio-dump leaching, where the ore is placed in a sealed pit and irrigated with a leaching solution (Natarajan, 2018).

In the 1980s, biooxidation started to be applied to the pretreatment of gold ores (mainly arsenic pyrite and pyrite) to release gold from the mineral matrix. The process leaches gold

indirectly by breaking down the sulfide shell around it to make it accessible for cyanide treatment (Jorjani & Askari Sabzkoohi, 2022). In the present day, there are novel directions in the bioleaching technology; the metals of interest have broadened to REEs and novel substrates, like electronic waste, can now be targeted. The focus has also shifted to valorizing ore reserves and wastes, where conventional methods are not economically feasible.

Bioleaching is an environmentally friendlier approach to leach metals than hydro- or pyrometallurgical methods by abstaining from the use of high temperatures and the use and production of toxic compounds. Microorganisms can even detoxify the substrate by transforming the toxins into less harmful forms or by immobilizing them. For example, some bacteria oxidize toxic arsenic III (AsIII) to a more harmless form – ferric arsenate or oxidized arsenic in amorphous compounds, which precipitates and can be removed in the process (van Aswegen *et al.*, 2007). Certain sulfate-reducing bacteria can be used to reduce metal ions such as Cd^{2+} and Pb^{2+} into insoluble sulfides (CdS, PbS), which precipitate out, *e.g.* from contaminated water and later can be utilized accordingly (Gu *et al.*, 2020). Another way is the sorption of toxins on the cell walls and transport into the cells, which don't get rid of the toxin, but keep it contained. The cells could then be removed by centrifugation or filtering.

Bioleaching efficiency is influenced by several physicochemical properties and conditions: the nature of the substrate, the organism used, the culture medium, pH, temperature, and aeration. In most cases, the substrate is ground into a fine fraction, with a particle size of approximately 1 mm, to increase the surface area of the particles. A larger surface area enhances leaching efficiency by providing more opportunities for reactions, such as allowing more area for cells to attach and acids to interact. However, excessively small particle size can hinder leaching efficiency due to bioaccumulation before bioleaching (Amiri *et al.*, 2012). Particles absorbed by the cells are essentially removed from the leachable substrate, thus lowering the maximum amount that could otherwise be leached. Temperature must be selected considering the optimal growth conditions for microorganisms, along with the thermal stability of the media and substrate. Whether the culture is aerobic or anaerobic, contact with oxygen needs to be managed by either providing a sufficient flow of air (aerobic) or ensuring proper isolation to prevent oxygen toxicity (anaerobic). The medium can significantly impact the metabolites secreted by the microbes. The sources of carbon and nitrogen, as well as their ratio (C/N ratio), greatly influence organic acid production and cell division rates, which is discussed more in the acidolysis chapter. Limiting certain elements in

the medium, such as phosphorus or iron, can aid bioleaching due to the microorganisms producing metabolites, such as organic acids, to scavenge the limited elements (D. Odoni, 2017). Said metabolites are secreted and can chelate the limited element (for example iron), and are then taken up by the cells with the chelated element.

Bioleaching can occur in extreme conditions, due to a low pH (around 2) or a relatively high metal content, which can be toxic to living organisms (R. Liu & Zhou, 2022). Acidophiles and chemoautotrophs are widely used precisely for their ability to bioleach and at the same time tolerate extreme circumstances (pH, metal content). However, these characteristics are not essential when the cells are used for continuous production of biolixiviant, separate from the reaction environment containing the metal-bearing substrate (Antonick et al., 2019). Biolixiviant is produced when cells grow in the medium for a certain period. While the cells may or may not have been removed, this biolixiviant (also known as spent medium) contains the metabolic compounds that the cells have excreted, such as organic acids.

In addition to chemoautotrophs, there are several other types of microorganisms used in bioleaching applications, such as heterotrophic bacteria, yeasts, archaea, algae and filamentous fungi. Species from the genus *Aspergillus* have garnered especially high interest due to their high production of organic acids. *Aspergillus niger* is the most studied among them, compared for example to its close relative *Aspergillus japonicus* in regard to bioleaching and acid production. *A. niger* has been commercially used in the production of citric, oxalic and gluconic acid, which are also effective lixiviants for the leaching of ores (Dronawat *et al.*, 1995; Grewal & Kalra, 1995; Strasser *et al.*, 1994). The organic acid secreted at the highest concentration by *A. niger* is gluconic acid at 13,7 g/L after 15 days of cultivation, with the concentration peaking at day 9 (Ren *et al.*, 2009). In the study by Ren *et al*., it was determined that gluconic and citric acid achieved higher leaching efficiencies than oxalic and malic acid. In addition, they found that different acids leached different metals, with gluconic acid removing more Cd and Pb, while citric acid removed more Cu and Zn from contaminated soil. Another study found that the organic acids secreted by *A. niger* can form complexes with REEs found in ionic rare earth ore (Wang *et al.*, 2025).

1.2.1. Redoxolysis

Redoxolysis in bioleaching includes oxidative and reductive bioleaching, with oxidative being most commonly used and reductive bioleaching is less common (Dong *et al.*, 2023; Vera *et al.*, 2022). The chemoautotrophic bacteria used in redoxolysis can oxidize metals in their electron transport chain (ETC). For example, iron-oxidizing bacteria generate energy by oxidizing Fe^{2+}, the electrons are donated to oxygen, which is then reduced. The oxidized iron(III) in turn can oxidize *e.g.* a metal sulfide in the substrate, causing a metal cation to release from the sulfur compound (Vera *et al.*, 2022). The iron is reduced by the previous process and can be used again as an electron donor in the ETC.

The Fe^{3+} ions and H^+ protons produced by the microorganisms described enhance the breakdown of sulfide minerals in the ore. The chemical bond between the metals and sulfide anion is broken and the metal is released into solution. Sulfide minerals are oxidized by two pathways: the polysulfide and thiosulfate pathways (Jones & Santini, 2023). The pathway is determined by the electron configuration in the sulfide mineral. In the polysulfide pathway, acid-soluble minerals, such as chalcopyrite ($CuFeS_2$), are attacked by protons (Figure 1). In acidic conditions, the metal-sulfur bonds are broken by protons and hydrogen sulfide is formed. Ferric iron (Fe^{3+}) causes H_2S^+ to form, before it spontaneously dimerises to H_2S_2. H_2S_2 is oxidized by ferric ion to elemental sulfur, which can be oxidized to sulfuric acid (SO_4^{2-}) by microbes.

$$MS + Fe^{3+} + H^+ \rightarrow M^{2+} + 0.5\ H_2S_n + Fe^{2+} \text{ (where } n \geq 2)$$
$$0.5\ H_2S_n + Fe^{3+} \rightarrow 0.125\ S_8 + Fe^{2+} + H^+$$
$$0.125\ S_8 + 1.5\ O_2 + H_2O \rightarrow SO_4^{2-} + 2\ H^+$$

Figure 1. Polysulfide pathway. M - metal. Protons (H^+) and ferric iron (Fe^{3+}) cause the metal-sulfide mineral oxidation and formation of sulfuric acid. (Jones & Santini, 2023)

Acid-insoluble minerals, such as pyrite, are oxidized in the thiosulfate pathway, in which thiosulfate ($S_2O_3^{2-}$) is generated via ferric iron (Fe^{3+}) and H_2O (Figure 2). The thiosulfate is rapidly oxidized by ferric iron, resulting in the production of tetrathionate (S_4O^{2-}), which degrades to several compounds, the prevalent one being sulfuric acid (SO_4^{2-}).

$$FeS_2 + 6\ Fe^{3+} + 3\ H_2O \rightarrow S_2O_3^{2-} + 7\ Fe^{2+} + 6\ H^+$$
$$S_2O_3^{2-} + 8\ Fe^{3+} + 5\ H_2O \rightarrow 2\ SO_4^{2-} + 8\ Fe^{2+} + 10\ H^+$$

Figure 2. Thiosulfate pathway. Ferric iron (Fe^{3+}) oxidizes metal sulfides and causes the formation of sulfuric acid. (Jones & Santini, 2023)

These organisms fix CO_2 in the Calvin cycle and don't need additional organic carbon, which significantly lowers the cost of the leaching process. Common chemoautotrophic bacteria used in oxidative bioleaching are *Acidithiobacillus ferrooxidans, Acidithiobacillus thiooxidans* and thermoacidophilic archaea of the archaeal order *Sulfobales* (Manesh *et al.*, 2024; Vera *et al.*, 2022). The thermoacidophilic archaea are capable of oxidizing ferrous iron and reduced inorganic sulfur compounds, utilizing the energy through the ETC (Manesh *et al.*, 2024). The higher growth temperatures of around 60-80°C needed for these archaea may aid in bioleaching kinetics. The temperature affects the reduction potential of various sulfur, iron and cuprum compounds, even changing the hierarchy between them, for example Fe^{3+} to Fe^{2+} reduction is more favorable at 70°C than 30°C, which may shift the sulfur and iron oxidation rate balance (Manesh *et al.*, 2024).

Reductive bioleaching encompasses the dissolution of material by a chemical reduction reaction catalyzed by microorganisms. For example, *Shewanella putrefaciens* is used to reductively dissolve jarosite ($MFe_3(SO_4)_2(OH)_6$) and gossan minerals (Castro *et al.*, 2017). *S. putrefaciens* utilizes Fe(III) in the jarosite to oxidize lactate and pyruvate, causing the reduction of iron. Iron reduction can also be mediated by sulfur-oxidizing acidithiobacilli under low pH, and some *Acidithiobacillus ferrooxidans* strains have been found to use the respiratory chain components of the iron oxidation in reverse (Malik & Hedrich, 2022).

1.2.2. Acidolysis

Acidolysis encompasses the dissolution of metals from ore through acids and protons produced by microorganisms. Chemoautotrophic acidophiles acidify and need an acidic environment for ATP production. The low pH outside of the cell provides a strong proton motive force used by ATP synthase to convert the spontaneous flow of protons across the cell's membrane to chemical energy. The high concentration of H^+ protons that enter the cell through chemiosmosis could lead to the pH in the cytoplasm dropping below a critical value (Alberts *et al.*, 2002). To avoid cytoplasmic acidification, ATPases can be Na^+ linked (instead of H^+) and/or H^+ can be removed by the proton pump or collected in vesicles and expelled from the cell. The chemoautotrophs, such as *A. ferrooxidans*, produce sulfuric acid by oxidizing sulfur compounds, mediated by Fe^{3+} as described in the redoxolysis chapter. The protons provided by sulfuric acid can break sulfide bonds in the ore, releasing the metal in the process.

Acid bioleaching utilizing heterotrophic bacteria and fungi is a widely studied indirect mechanism. These organisms need an added carbon source like glucose, making the process considerably more expensive than with chemoautotrophs. On the flipside, these organisms have far faster growth rates than chemoautotrophs. The microorganisms produce organic acids, resulting in a lowered pH and complexation of metals. Protons aid in metal solubilization by reacting with oxygen on the material's surface and organic acids can chelate metal ions (see 1.2.3. Complexolysis) (Srichandan *et al.*, 2019). The reduced pH promotes the substrate particles' surface destruction, the metals (including REEs) dissociate from the mineral phase and may interact with organic acids.

Organic acid production in *A. niger* is mostly influenced by the concentration of the carbon and nitrogen sources and their ratio, as well as Mn, Fe and P concentrations, the biomass and parameters like temperature and dissolved oxygen (D. Odoni, 2017; Sankpal & Kulkarni, 2002). A high C/N ratio tilts the cell's metabolism towards energy production (glycolysis), and a low C/N ratio boosts biosynthesis (TCA cycle, amino acid production). High C/N ratio and nitrogen limitation have been thoroughly studied in the oleaginous yeasts such as *Yarrowia lipolytica* (Beopoulos *et al.*, 2009; Cavallo *et al.*, 2017; Ledesma-Amaro & Nicaud, 2016). During nitrogen limitation, adenosine monophosphate (AMP) deaminase is activated, reducing the concentration of AMP in the cell and producing IMP and NH_4^+ (Beopoulos *et al.*, 2009; Evans & Ratledge, 1985; S. Li *et al.*, 2024). IDH is allosterically activated by AMP; therefore, with lower levels of AMP, IDH is inhibited (Hathaway & Atkinson, 1963; Kornberg & Pricer, 1951). This leads to TCA arrest at the isocitrate level, which can be converted into citrate. While less studied than in yeast, the same mechanism is believed to operate in filamentous fungi. Citrate exits the mitochondria through the citrate/malate cycle. In oleaginous yeasts, the ATP-citrate lyase (ACL) cleaves citrate, forming oxaloacetate and acetyl-CoA, the latter of which is used for fatty acid synthesis (Beopoulos *et al.*, 2009). In *A. niger*, it has been proposed that ACL enzymes take part in a futile cycle consuming ATP for energy balance when citric acid is produced (Yin *et al.*, 2017).

The *Aspergillus* genus produces large quantities of organic acids, like fumaric and malic acid, under specific stress conditions (Goldberg *et al.*, 2006). These TCA cycle intermediates are produced by the reductive TCA pathway, localized in the cytosol (Figure 3) (Khandelwal *et al.*, 2023). Certain filamentous fungi, including *A. niger*, harbor cytosolic pyruvate carboxylase, malate dehydrogenase and fumarase (Knuf *et al.*, 2013). These are key enzymes in the

accumulation of fumaric and malic acids. Nitrogen limitation is the primary stress condition that causes the fungi to produce the mentioned acids instead of biomass (Knuf *et al.*, 2013). N-starvation leads to additional fumarate production through the urea cycle in the filamentous fungus *Rhizopus delemar* (D. Odoni, 2017). It was found that in high fumarate producing conditions, in addition to overexpression of TCA cycle enzymes pyruvate carboxylase (PYC), malate dehydrogenase (MDH) and fumarase (FumR); argininosuccinate lyase (ASL), an urea cycle enzyme, was overexpressed as well (D. Odoni, 2017). This indicates that under nitrogen starvation, amino acids are catabolized, leading to excess production of fumarate through the urea cycle.

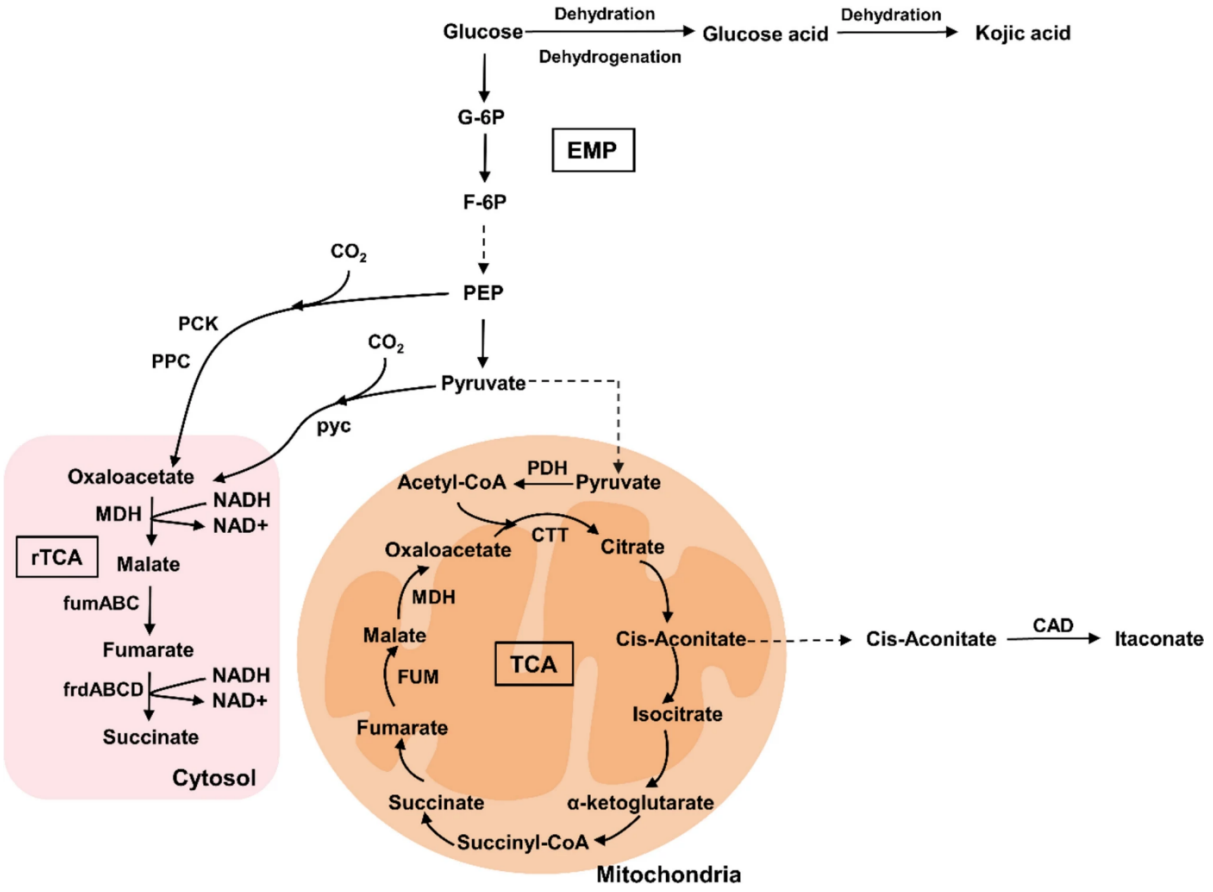

Figure 3. Organic acid metabolic pathways in *Aspergillus*. Author: (Y. Wu *et al.*, 2025)
The production of malate and fumarate occurs in reductive TCA (rTCA) shown in pink. Citrate is primarily made in the mitochondrial oxidative TCA cycle.

Citric acid accumulates in the mitochondrial oxidative TCA pathway, however, the cytosolic malic acid is an intermediate in citric acid biosynthesis. Citric acid accumulation in *Aspergillus* can be evoked by high carbohydrate concentration, low concentrations of certain elements, high dissolved oxygen, constant agitation and low pH (Goldberg *et al.*, 2006; D. I. Odoni *et al.*, 2017). Increased glucose concentration upregulates a major citric acid exporter CexA, along

with most of the genes involved in glycolysis in *A. niger* (Zheng *et al.*, 2023). The study also found that most TCA cycle-related genes were upregulated during glucose depletion. The production of citric and other acids under stress conditions aids the fungi in several ways. Environmental acidification leads to lower pH, which can inhibit the growth of competing microorganisms and help to solubilize nutrients such as phosphate in the environment (Knuf *et al.*, 2013). The production of organic acids regulates metabolic balance by removing excess carbon, in the case of limited nitrogen or phosphate content. Organic acids can be used in scavenging metals by chelating them, for example, *A. niger* secretes citrate to increase iron bioavailability (D. Odoni, 2017).

1.2.3. Complexolysis

The primary organic acids, that have been found to form metal complexes and chelates are citrate, oxalic acid, tartaric acid, L-ascorbic acid, malonic acid, malic acid and maleic acid (Dusengemungu *et al.*, 2021; P. Liu *et al.*, 2025). The organometallic complexes are soluble at low pH levels. The complexation of metals to organic compounds, which stabilizes the metal ions, minimizes the toxic effect of the metal ions on fungi.

Amino acids can also form complexes with metals, but their secretion by fungi is rare. Glycine is the most studied amino acid in extractive metallurgy due to its low cost and availability in large industrial quantities (H. Li *et al.*, 2023). The metal ions are often oxidized or reduced before complexing with glycine. The leaching is usually done by using glycine solution directly, not by cultivating microbes to produce the amino acid. However, some bioleaching experiments have found that intrinsically synthesized amino acids may play a role in leaching. *Arthrobacter creatinolyticus* has been found to leach gallium (Ga) from GaN by several excreted amino acids (Maneesuwannarat *et al.*, 2016). Increased leaching efficiencies by amino acids were found under higher pH values: at pH=9 lysine 56%, aspartic acid 50%, glutamic acid 49 % and arginine 39% (Maneesuwannarat *et al.*, 2016). This is likely due to the amino acids having an increased negative charge at higher pH's. The positively charged metals bind with the negatively charged amino acids more efficiently.

Several organic ligands can form complexes with metals in addition to amino acids and organic acids; important groups of molecules are cyanide and siderophores (Christenson & Schijf, 2011; R. Liu *et al.*, 2016; Wen *et al.*, 2024). Cyanogenic microbes (organotrophs), including

bacteria and a few fungal species, produce a potent respiratory inhibitor, hydrogen cyanide (HCN) from glycine (Srichandan *et al.*, 2019). The reason for this is believed to be competition with other microbes and defense against predators. Cyanide can also react and form complexes with many highly inert metals, from which gold, silver and platinum particularly are under scientific interest (Figure 4).

$$4\ Au + 8\ CN^- + O_2 + 2\ H_2O \rightarrow 4\ Au(CN)_2^- + 4\ OH^-$$

Figure 4. Gold dissolution in cyanide solution. (R. Liu *et al.*, 2016)

Siderophores are metal-binding molecules secreted by several bacteria and fungi, that typically chelate iron with high affinity (Neilands, 1995). Some siderophores have been found to have a strong affinity towards other trivalent metal cations (besides Fe(III)), which includes most REEs in their usual form, except for Ce^{4+} and Eu^{2+}. Desferrioxamine B (DFOB), native to *Streptomyces pilosus,* is the most studied siderophore that outcompetes carbonate for chelating REEs (Telfer *et al.*, 2019; Wen *et al.*, 2024).

1.2.4. Bioleaching of phosphate rocks by filamentous fungi

Phosphate rock can be solubilized with organic acids by increasing the concentration of protons (H^+) and due to their chelating ability. The organic acids can combine with metal ions, including Ca^{2+}, which facilitates the phosphate solubilization from apatite ($Ca_5(PO_4)_3(F,Cl,OH)$) (Holah *et al.*, 2019). REEs, which substitute the Ca^{2+} in apatite, can be leached in this way as well, by forming complexes with organic acids (Holah *et al.*, 2019; Xiqiang *et al.*, 2020). Certain organic acids can selectively extract REEs from solution in the later steps of processing with efficiencies up to 99,76% (P. Liu *et al.*, 2025).

Phosphate-solubilizing fungi (PSF) have primarily been studied for their benefits to plants, as they enhance phosphate availability in the soil by solubilizing inorganic phosphate. The ability of *Aspergillus* species to solubilize inorganic phosphate in the presence of different energy and carbon sources and metals has previously been studied. Seshadri *et al.* (2004) described the effect of nitrogen and carbon sources on the ability of *A. niger* to solubilize inorganic phosphate. The study found that although all *A. niger* strains were able to solubilize all phosphate sources tested, solubility was poorer for aluminum and iron-based phosphates compared to di- and tricalcium phosphates, and the results varied with different *A. niger*

strains (Seshadri *et al.*, 2004). This suggests that different strains undergo physical changes in how they dissolve inorganic phosphate and handle metals, and the physical changes are influenced by their original growth environment.

The toxicity of heavy metals to PSFs isolated from the rhizosphere of common reed, including *A. niger* and *A. japonicus*, has also been previously examined (Zúñiga-Silva et al., 2016). In the aforementioned study, it was found that the phosphate solubilization index (PSI) of the filamentous fungi used in the experiments is influenced by the concentration of metals in the environment, and the type of metal plays an important role. As the concentrations of almost all metals used in the experiments (Al, Cd, Co, Cr, Cu, Ni, Pb, and Zn) increased, the phosphate solubilization capacity of *A. japonicus* also increased—except for nickel, where PSI remained constant, and lead, where it varied at different concentrations. The work by Zúñiga-Silva and colleagues compares the results obtained with those of other authors and concludes that tolerance to metals depends on the previous growth location of the fungus, as they may have developed physiological adaptations to tolerate metals (Zúñiga-Silva et al., 2016).

The pH of the solution is one of the most important parameters that determines the efficiency of phosphate solubilization by filamentous fungi. PSFs produce organic acids such as citric acid, oxalic acid, lactic acid, and malic acid, which help to make phosphates more bioavailable by acidifying the environment and chelating phosphate-bound cations. Organic acids can form coordination compounds or coordination complexes with metals that are bound to phosphate. PSFs can also utilize phosphatases, which are phosphate-hydrolyzing enzymes.

The main mechanism of phosphate solubilization in *A. japonicus* is believed to be the production of organic acids. The following organic acids are produced by *A. japonicus* after 3 weeks of incubation in decreasing order of concentration: ascorbic acid, oxalic acid, formic acid, malic acid, succinic acid, lactic acid, and citric acid (Mahgoub *et al.*, 2022). Another study measured organic acid production for the first 7 days by *A. japonicus* and found that acid production varies in time, with gluconic acid being predominantly produced, followed by oxalic acid, and ascorbic acid wasn't detected until day 6 (Xiao *et al.*, 2018). Both studies used National Botanical Research Institute's Phosphate (NBRIP) medium and rock phosphate; however, there were differences in the amount and concentration of inoculum used, additives, and growing conditions such as temperature and moisture content. Another mechanism for lowering pH besides organic acid production includes the release of protons following respiration or NH_4^+ assimilation (Xiao *et al.*, 2018).

The previous text might give the impression that when more acid is produced, *i.e.*, the pH of the solution lowers, the more phosphate dissolves. However, organisms have certain limits on how low a pH they can tolerate and grow in*, A. japonicus* has a growth optimum at around pH=7 and is known to be able to grow and solubilize phosphate in the pH range of 4-11, but this range may also extend to lower pH levels that have not been tested. Periodically adjusting pH to around 7 may improve leaching efficiency, as fungal growth is inhibited at lower pH levels (Xiao *et al.*, 2011). The leaching efficiency could increase due to the more optimal growth of the fungi, leading to more biomass and thus higher acid production.

The effect of alkaline conditions on *A. japonicus'* ability to solubilize phosphorus from rock phosphate is inhibitory, due to the fungi's hindered growth (Singal *et al.*, 1994). The study indicates that phosphorus solubilization by *A. japonicus* is slightly enhanced in the presence of pyrite, likely due to the fungi's ability to oxidize the pyrite. This leads to the formation of sulfuric acid, which contributes to the increased solubilization of phosphorus under alkaline conditions. A summary of studies on phosphate solubilization using *A. japonicus* can be found in Table 1.

It has been suggested that a vital role in phosphorus solubilization is the attachment of fungal cells to the surface of the substrate, which helps to break down the material (Xiao *et al.*, 2018). In studies where *A. japonicus* and abiotic solutions with organic or inorganic acids were compared; the abiotic solutions had lower rates of soluble phosphate released (Xiao *et al.*, 2011, 2018). The morphology of fungi growing in liquid media varies; the fungi can grow in filamentous form with homogeneously dispersed hyphae or form spherical pellets consisting of aggregated hyphal structures (Veiter *et al.*, 2018). The main triggers for pellet formation are electrostatics, hydrophobicity and interactions between spore wall components (Veiter *et al.*, 2018). Alterations in morphology may be triggered by strong agitation, low pH, aeration and inoculum level (Zhang & Zhang, 2016). The spores typically have a negative charge, so aggregation is favorable at lower pH values, and the pH can also affect the hydrophobicity of proteins (hydrophobins) on the cell wall (Veiter *et al.*, 2018; Zhang & Zhang, 2016).

1.2.4.1. The media used for PSF cultivation

The main media used for culturing PSFs in the laboratory are Pikovskaya (PVK) and National Botanical Research Institute's Phosphate (NBRIP) media, both of which contain tricalcium phosphate ($Ca_3(PO_4)_2$) as a phosphate source (Nautiyal, 1999). In addition to $Ca_3(PO_4)_2$, NBRIP contains glucose, $MgCl_2$, $MgSO_4$, KCl, and $(NH_4)_2SO_4$, and PVK contains glucose, $MgSO_4$, KCl, $(NH_4)_2SO_4$, NaCl, $MnSO_4$, $FeSO_4$ and yeast extract. PVK allows qualitative assessment of phosphate solubility, and NBRIP is used for both qualitative and quantitative analysis. On PVK agar, as phosphate dissolves, a transparent ring forms around the colony, leaving the rest of the medium white. NBRIP media has a similar effect (Nautiyal, 1999). However, this medium is preferred for qualitative analysis because, unlike PVK, it is a minimal medium, giving more stable test results.

Chapek Dox agar is a semisynthetic medium used to isolate and cultivate fungi, including *Aspergillus*. Chapek Dox media has also been used previously to study the effects of phosphate solubilization by several fungi, including *A. niger*, a close relative to *A. japonicus* (Saxena *et al.*, 2013). Although in the study it was concluded that PVK media is better suited for phosphate solubilization, it was mentioned that one of the reasons for this phenomenon might be that NH_4^+ in PVK is a better source of nitrogen than NO_3^- in Chapek Dox media.

Malic and fumaric acid production by *Aspergillus oryzae* has been previously studied with different carbon sources (glucose, xylose and glycerol) and different C/N ratios (300:1, 200:1 and 100:1) (Ochsenreither *et al.*, 2014). In those experiments, it was found that all carbon sources can be used for malic and fumaric acid production, but the production is highest with glucose. It was also demonstrated that organic acid production was highest with a 300:1 C/N ratio.

Table 1. Summary of studies done on phosphate biosolubilization using *A. japonicus*.

Source	Substrate type	Composition (total P)	Substrate in experiment	Medium	Temperature	rpm	initial pH	Modifications	Phosphate solubilized
(Singal *et al.*, 1994)	Indian low-grade Rock Phosphate (Ca-P)	N/A	0,5% w/V	Pikovskaya medium	30° C	static	8/9	0,1% w/v Pyrite in experiments	53,65% with pyrite and pH 8 48,2% without pyrite and pH 8
(Xiao *et al.*, 2018)	Rock Phosphate from China (Ca-P)	8,35% Phosphorous in RP	0,2% w/V. 382,69 mg/L P_2O_5 Ground to 100-200 mesh.	NBRIP medium with 1% glucose	30° C	140	7	N-sources tested: $(NH_4)_2SO_4$, NH_4Cl, NH_4NO_3, KNO_3, $NaNO_3$ and $Ca(NO_3)_2$	135,2 mg/L which corresponds to 35,3%
(Xiao *et al.*, 2011)	Rock Phosphate from China (Ca-P)	N/A	1% w/V. Ground to 100-200 mesh.	NBRIP medium with 1% glucose	30° C	160	7	Different conditions tested: temperature (10-35), pH (4-11) and salinity (0-3,5%).	89,53 mg/L which corresponds to approximately 23,4% (assumed that 8,35% P in RP)
(Mahgoub *et al.*, 2022)	Rock Phosphate (Ca-P)	7,97% Phosphate in RP	0,31% w/V 250 mg/L P_2O_5	NBRIP medium with 1% glucose	28° C	150	7	Solid state fermentation included	30,15 mg/L which corresponds to 12%
(Tian *et al.*, 2014)	$Ca_3(PO_4)_2$	61,2% Phosphate in $Ca_3(PO_4)_2$	0,2% w/V (2000 mg/L)	Pikovskaya medium with 1% C-source	N/A	N/A	7	Tested various C- and N-sources	2000 mg/L which corresponds to 100%

1.2.4.2. *Aspergillus japonicus*

Aspergillus japonicus is a species of fungi belonging to the family *Aspergillaceae* and the phylum *Ascomycota* (Schoch *et al.*, 2020). *Aspergillus japonicus* was first identified and named by a Japanese mycologist, K. Saito, in 1906. The fungus was described to form "a thick, initially white, soon black-brown biomass on the media" (Saito, 1906). The genus *Aspergillus* was named after a holy water sprinkler because of the similarity in shape in 1729 by an Italian priest and biologist, Pier Antonio Micheli. *Aspergillum* means holy water sprinkler in Latin, it is derived from *spargere,* meaning to sprinkle. *Japonicus* stands for "from Japan" or "Japanese" in Latin, which refers to the place Saito isolated it from – the soil in Japan.

Aspergillus, as a genus, has a diverse metabolism and has been found in a variety of different habitats – the desert, salt marshes, the Pacific Ocean, the Arctic, crop fields, Eastern Himalayas, mummified human remains, etc (Abdel-Azeem *et al.*, 2019). Species in the genus *Aspergillus* produce asexual spores (conidia), for *A. japonicus* these can be seen as black dots in contrast to the white-ish biomass. The dark pigmentation of the spores is common in the *Nigri* group of the *Aspergillus* genus, to which *A. japonicus* has been grouped in some phylogenetic studies (Steenwyk *et al.*, 2024; Yokoyama *et al.*, 2001). The optimal growth for *Aspergillus* species occurs at temperatures between 25-37°C. *A. japonicus'* genome, with a size of 36.1 Mb, has been assembled at the scaffold level and published in the GenBank database in June 2018 (NCBI, 2018). The genome has a GC percentage of 51% and 12 015 protein-coding genes.

The ability of *A. japonicus* to secrete organic acids and effectively solubilize inorganic phosphate, including from rock phosphate, has been thoroughly researched. *A. japonicus* can tolerate acidic conditions of at least around pH=4, if not lower, which enhances rock phosphate dissolution (Xiao *et al.*, 2011). *A. japonicus* is also generally recognized as safe, meaning it is suitable for use in agricultural applications.

1.3. Industrial bioleaching solutions

Bioleaching operations can be conducted in different scales: 1) small: shake flasks 2) intermediate: stirred tank and column reactors and 3) commercial: agitated tank reactors, heap and dump.

1.3.1. Stirred reactors

Stirred bioreactors are used to perform intermediate-scale operations to simulate the commercial-scale agitated tank. The reactors offer a controlled environment for metal recovery, where temperature, aeration and stirring speed can be controlled as desired. However, the agitators and pumps for continuous stirring and aeration as well as temperature control, consume a significant amount of energy. Additionally, the tank reactors have a low solid-to-liquid ratio.

At the Fairview Gold Mine in Africa, agitated tank bioleaching of sulfide concentrates was developed in 1986 (Gericke *et al.*, 2009). The Fairview plant uses the BIOX^{TM} process, which uses biooxidation of the ore by a mixed culture of acidophilic bacteria (van Aswegen *et al.*, 2007). These bacteria oxidize the sulfide minerals in the gold concentrate, converting them into soluble ferric and sulfate compounds, thereby exposing the gold for cyanidation.

Tanks are used in cobalt leaching as well, in 1998 the Kasese Cobalt Company inoculated their first tanks to leach cobalt from Kasese pyrite in Uganda (Morin & d'Hugues, 2007). The ore oxidation is driven by iron- and sulfur-oxidizing bacteria. The leaching is done in five reactors, with 3 being parallel primary reactors and 2 being used as secondary reactors, where the ore from the primary reactors is used. Approximately 60% of the pyrite is oxidized in the primary reactors and 20-30% in the secondary reactors (Morin & d'Hugues, 2007).

1.3.2. Stacked column

Column bioleaching is conducted in a vertical column that is packed with ground ore (Srichandan *et al.*, 2020). The leaching solution is applied at the top, percolates through the column and leachate is collected at the bottom, from which pH and concentration of solubilized metals may be analyzed. The key advantage compared to tank reactors is the increased solid-to-liquid ratio, which leads to higher reaction efficiencies due to enhanced contact between reactants in the liquid and the solid phase. Additionally, the stacked column consumes less energy, as there is no constant stirring in the process. In addition to bioleaching, stacked columns, also known as packed bed reactors, are widely used in other applications such as wastewater treatment, catalytic reactions and gas absorption.

A laboratory operation mimicking column leaching is a semi-continuous culture in a shake flask test that can be used for screening and optimization before leaching in columns (Xia *et al.*, 2013). The setup mimics aspects of column leaching, while allowing a controlled environment and rapid testing with lower costs. The leachate can be removed periodically and replaced with fresh medium, keeping the same ore and biomass. The leachate can be used for monitoring pH, metal concentrations and microbial activity (CFU, acid production).

In a stacked column, multiple columns are arranged (stacked) sequentially and the leaching solution flows from one column to the next. This setup simulates the multi-stage leaching effect in heap-leaching, where the ore and microbial biomass are more heterogeneous throughout the heap. Continuous column bioleaching experiments with *A. ferrooxidans* and sulfide ore material to simulate heap-leaching were done in Finland as early as 1986, with metal recoveries of Zn 25%, Cu 8%, Ni 44% and Co 18% (Puhakka & Tuovinen, 1986).

1.3.3. Heap bioleaching

Heap bioleaching has been researched since the 1950s and a copper mine using bacterial leaching started operating in Potrerillos, Chile in the early 1970s (Tanaka, 2017). Commercial heap-leaching operations, primarily copper from chalcopyrite, are of sufficient scale to process thousands of tons of ore per day (Brierley, 2001; Pradhan *et al.*, 2008). Heap leaching is a large-scale operation that uses lixiviant percolation on crushed ore on prepared leach pads (Figure 5 and 6). The mined ore is usually crushed beforehand to below 25 mm and usually agglomerated before being hauled to the leach pads (Natarajan, 2018). Agglomeration is necessary to provide the efficient flow of the lixiviant, otherwise, the fine-grained particles may occupy the spaces between the ore fragments and simply block the flow (Bleiwas, 2012). The crushing of the ore is necessary to increase the surface area that is accessible to microbes and can react with their metabolites. The leaching solution percolates through the porosity of the rocks and is collected after draining for metal recovery. The heap method provides a heterogeneous environment for microbes, with varying pH, temperature, aeration and liquid composition within the heap (Natarajan, 2018). Heap-leaching has lower costs than tank reactor leaching due to a high solid-to-liquid ratio and lower energy needs, as described in the stacked column chapter.

Terrafame in Sotkamo is one of the world's largest industrial-scale heap bioleaching plants, processing a polymetallic black schist ore. It produces large quantities of cobalt, estimated at 500 tonnes annually, positioning 25th on the global scale by the amount of cobalt produced (Tuomela *et al.*, 2021). In addition, the Sotkamo mine also produced 28 582 tonnes of nickel and 54 353 tonnes of zinc in 2021 (Heikkinen *et al.*, 2022). The mineral resources are mined in a large-scale open pit mine at Kuusilampi. The ore is crushed in several stages and agglomerated in a rotating drum before it is conveyed and stacked on heap pads. The heap-leaching process at Terrafame is divided into two stages. The primary stage contains about 24 to 28 tonnes of ore and takes approximately 15 months and the secondary stage uses partially leached ore from the primary stage to enhance metal release (Heikkinen *et al.*, 2022). The leaching solution contains sulphuric acid and has a low pH at 2,0-2,5 and the leaching of metals is catalyzed by bacteria such as *A. ferrooxidans* (Riekkola-Vanhanen, 2013; Tuovinen *et al.*, 2018). After leaching, Cu, Zn, Ni and Co are precipitated and filtered from the pregnant leaching solution (Figure 5 and 6). The leaching solution is then purified further and used again to percolate the heap. Terrafame began uranium extraction at the Sotkamo mine in 2024 (Ministry of Economic Affairs and Employment of Finland, 2024).

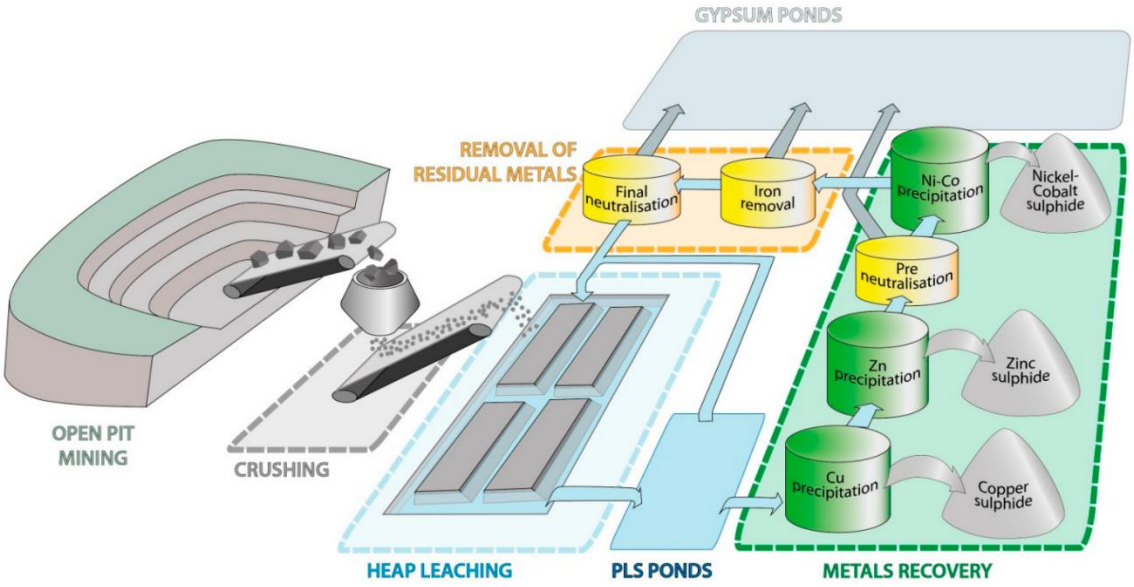

Figure 5. Heap leaching scheme at the Terrafame (previously named Talvivaara) plant. PLS - Pregnant leaching solution. Author: (Tuovinen *et al.*, 2018)

Figure 6. Bioheaps at Terrafame (previously named Talvivaara) in 2015. Author: (Yle, 2015)**.**

2. EXPERIMENTAL PART

2.1. The aims of the thesis

The aims of the thesis are to:

1. Optimize a medium for bioleaching phosphorite with *Aspergillus japonicus*.

2. Determine the leaching efficiency of phosphorus, REEs and uranium from Estonian phosphorite by *A. japonicus*.

2.2. Materials and methods

2.2.1. Substrate enrichment

The phosphorite was collected in northern Estonia as a hand specimen previous to the start of this project. The phosphorite consisted of shell fraction and sand fraction (Figure 7). Some of the sand fraction was removed from the phosphorite by sieving and grinding in a ceramic mortar to enrich the phosphorus content of the phosphorite. The phosphorite was first sieved, then the product was ground in a mortar and sieved again. To get finer substrate particles, the coarse concentrated fraction was ground one more time with mortar to produce a finer substrate, which was used in the experiments.

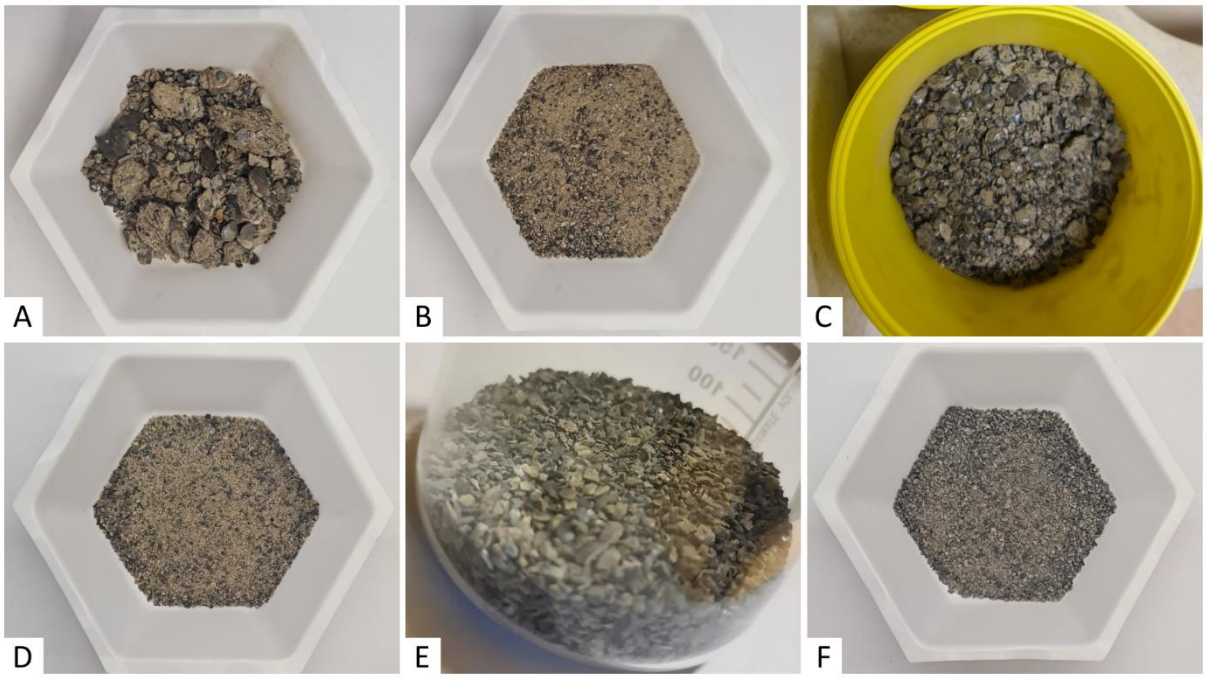

Figure 7. Pictures of phosphorite at different stages of enrichment. A. Starting substrate. Phosphorite before grinding and sieving. B. 1st fraction. The sand fraction that was removed by sieving. C.

Intermediate fraction. The unground phosphorite after removing 1st sand fraction. D. 2nd fraction. The sand fraction that was removed after grinding and sieving 2nd time. E. Coarse concentrated fraction. F. Ground concentrated fraction.

2.2.1.1. Acid digestion of concentrated fraction

To compare the phosphorites' composition before and after enrichment by grinding and sieving, acid digestion was used. A sample from the concentrated fraction was placed to a round-bottomed flask, to which 12 mL of 36% HCl and 4 mL of 65% HNO_3 were added. The mixture was heated with stirring in an oil bath (140 °C) for 45 minutes, then cooled to room temperature, transferred to a 100 mL volumetric flask, and diluted with type I pure water (MilliQ H_2O) to the 100 mL mark. The suspension was filtered through paper filter. The filter was dried overnight at room temperature and weighed; the mass of the insoluble part was calculated. This procedure was done in 3 replicates for the concentrated fraction and the 2nd fraction.

2.2.2. *A. japonicus* growth conditions

A. japonicus DSM 2346 was purchased from Leibnitz Institute DSMZ in Braunschweig, Germany. *A. japonicus* was rehydrated from the lyophilized form in potato dextrose broth prepared by boiling 200 g potatoes in 1000 ml MilliQ H_2O for 1 hour, after which the mixture was passed through a fine sieve and supplemented with 20 g/L of glucose. For potato dextrose agar (PDA) 15,0 g/L agar was added. Strain was rehydrated by adding 1 mL of potato dextrose broth to the stock glass tube. After 15 min incubation at room temperature 500 µL of culture solution was transferred to 5 mL PDA liquid media in 100 mL Erlenmeyer flask. After 4 days of cultivation at 30°C 180 rpm, in-house stock was prepared by plating 50 µL of liquid culture on a PDA petri dish. The Petri dish was incubated for 4 days at 30°C in a zip-bag. Spores were taken up to solution which contained 0,8% NaCl, 0,025% TWEEN20, 20% glycerol and MilliQ H_2O and stored at -80°C. Later *A. japonicus* was routinely grown on PDA for 4 days and used for following experiments.

2.2.3. Bioleaching experiments

While cultivating cultures at 30°C with 180 rpm agitation in Erlenmeyer flasks, all preparational works are performed in sterile conditions. Sterile National Botanical Research Institute's Phosphate growth medium (NBRIP) with the following composition: 0,15 g/L $(NH_4)_2SO_4$, 0,25 g/L $MgSO_4$, 0,50 g/L $MgCl_2$, 0,20 g/L KCl, 10 g/L Glucose and MilliQ H_2O, was prepared from the sterile stock solutions of 5 times concentrated NBRIP, 40% D-Glucose solution and filled with MilliQ H_2O to a final volume taking into consideration 10% (V/V) of inoculum. For inoculum, a 10^7 spores/mL spore solution was made from a 4-day-old *A. japonicus* culture, which was grown on a PDA plate. The spores were taken up to MilliQ H_2O by gently rubbing them from the agar. Hemocytometer (Buerker) and 10x magnification microscope (Olympus BX41) were used for counting the spores. According dilution was made using MilliQ H_2O to get 10% (V/V) 10^7 spores/mL of final inoculum.

For the experiments with different C/N ratios, NBRIP was prepared without $(NH_4)_2SO_4$. The pH of both NBRIP media was adjusted to 7 with NaOH. Ammonium sulphate was added from 100 g/L autoclaved stock solution. The initial NBRIP media had a C/N ratio of 146:1 with 0,15 g/L $(NH_4)_2SO_4$ and 1% glucose. In addition to initial media, C/N = 50:1; C/N= 100:1 and C/N= 200:1 were tested with 10% glucose by changing $(NH_4)_2SO_4$ amount to 4,4 g/L; 2,2 g/L and 1,1 g/L respectively.

Phosphorite was sterilized in Erlenmeyer flasks by autoclaving at 112°C for 15min prior to starting the experiments. All experiments were done in 3-4 replicates. All experiments had blanks with no addition of *A. japonicus,* with the same number of replicates as the experiment. Experiments were maintained in a rotator (Eppendorf, Innova s44i) at a rotation speed of 180 rpm and temperature 30°C. Semi-continuous experiments were centrifuged at 5000 rpm for 15 min, the lixiviant was decanted, and the remaining biomass and substrate were mixed with fresh media. A summary of the experiments' conditions can be found in Table 2.

Table 2. Bioleaching experiments. All experiments were kept at 30°C and 180 rpm with 1% (w/V) substrate concentration and 10% (V/V) Inoculum with 10^7 spores/mL.

Experiment number and name	Medium composition	$(NH_4)_2SO_4$ concentration	Volume, mL	Sampling days	Cycles
1- Initial experiment	$MgSO_4$ 0,25 g/L $MgCl_2$ 0,50 g/L KCl 0,20 g/L Glucose 10 g/L	0,15 g/L	50	0, 1, 2, 3, 7, 14, 21, 28	1
2- C/N ratio experiment	$MgSO_4$ 0,25 g/L $MgCl_2$ 0,50 g/L KCl 0,20 g/L Glucose 100 g/L	C/N=50 4,4 g/L	100	0, 1, 2, 3, 7, 14, 21, 28	1
		C/N=100 2,2 g/L			
		C/N=146 1,5 g/L			
		C/N=200 1,1 g/L			
3- Semi-continuous C/N=200 48h experiment	$MgSO_4$ 0,25 g/L $MgCl_2$ 0,50 g/L KCl 0,20 g/L Glucose 100 g/L	C/N=200 1,1 g/L	50	0, 1, 2, 3, 4 … 31	16
4- Semi-continuous C/N=50 48h experiment	$MgSO_4$ 0,25 g/L $MgCl_2$ 0,50 g/L KCl 0,20 g/L Glucose 100 g/L	C/N=50 4,4 g/L	50	0, 1, 2, 3, 4 … 31	16

2.2.3.1. Determination of phosphorus content

Phosphorus content in samples was determined as molybdovanadophosphoric acid spectrophotometrically (Michelsen, 1957). Phosphate reagent contained 1,65 M HNO_3, 7,1 mM NH_4VO_3 and 6,7 mM $NH_4Mo_7O_{24}$. Ammonium molybdate ($NH_4Mo_7O_{24}$) reacts to form molybdophosphoric acid ($H_3[PMo_{12}O_{40}]$), which then turns into the yellow colored vanadomolybdophosphoric acid ($H_3PMo_{11}VO_{40}$). To prepare a solution for the calibration plot 30% (V/V) phosphate reagent, 1%-6% of 1 mg/mL P_2O_5 solution and milliQ H_2O were mixed. The calibration curve with 6 points was plotted according to known concentrations (0,01-0,06 mg/mL) of P_2O_5 and the corresponding absorbance values that were measured spectrophotometrically (Biochrom Libra S22) at 454 nm.

To determine whether centrifuging the sample will increase the amount of phosphorus in sample solutions by breaking the fungal cells, an experiment was conducted to compare the amount of phosphorus measured. Three methods were tested: 1) 13 000 rpm, 2 minutes centrifugation 2) 5000 rpm, 2 minutes centrifugation and 3) Filtering with 0,2 um pore size filters. Each method was tested in triplicate and samples were collected on days 1-4. All samples were collected to Eppendorf tubes that contained 100 µL 2% HNO_3. The substrates' total phosphorus content was calculated from the solubilized part of the acid-digested phosphorite (chapter 2.2.1.1.).

2.2.3.2. Determination of metal content

Metal content in the leachate and initial phosphorite material (after acid digestion) is determined using the inductively coupled plasma mass spectrometry method (ICP-MS). Bioleaching efficiency is calculated based on the metal concentrations in the leachate solutions and in the acid-dissolved phosphorite material. Samples from bioleaching experiments for ICP analysis were centrifuged at 13000 rpm for 2 minutes and collected in acid-washed Eppendorf tubes, to which a final concentration of 3,14% (V/V) HNO_3 was added and placed in 4°C until analysis time. The substrates' total metal content was calculated from the solubilized part of the acid-digested phosphorite (chapter 2.2.1.1.).

2.2.3.3. Measurement of organic acid production

Samples for organic acid measurements were collected from the C/N ratio experiments by filtering the experimental solution through a 0,2 µm syringe filter and stored at -20°C until analysis time. Enzymatic Assay Kits from Megazyme were used for the measurement of these acids: gluconic (K-GATE), citric (K-CITR) and tartaric (K-TART) (Megazyme, no date). α-ketoglutaric acid was measured with Sigma-Aldrich's assay kit (MAK541) (Sigma-Aldrich, no date). Samples were analyzed according to the respective protocols. The POLARstar OMEGA (415-1480) microplate reader was used to measure absorbances.

2.2.4. Statistical analysis

Statistical analyses and graph generation were performed using GraphPad Prism version [10.4.2] (GraphPad Software, San Diego, CA, USA). Statistical analyses were performed using two-way analysis of variance (ANOVA) followed by Tukey's post hoc test for multiple comparisons. Differences with a p-value of <0.05 were considered statistically significant. Data are presented as mean ± 95% confidence interval (CI).

2.3. Results and discussion

2.3.1. Phosphorite composition

While the overall composition of phosphorite is well studied, the large degree of heterogeneity of this material required a precise determination of our fractions prior to leaching experiments. The phosphorite was enriched by removing sand with grinding and sieving (Figure 7). The results from acid digestion showed that the grinding and 2nd sieving significantly raised the soluble part of phosphorite. The concentrated fraction is more soluble, compared to the more insoluble 2nd fraction. The average soluble part for the 2nd fraction was 52,9% ± 6% and for the concentrated fraction it was 88,9% ± 3% (Figure 8). The phosphorus content of the solubilized part was measured spectrophotometrically (described in chapter 2.2.3.1.). Considering the heterogeneity of the substrate, acid digestion and phosphorus measurements were done in 3 replicates to get a better representation of the average composition. The estimated total P_2O_5 content per 1 g of phosphorite (concentrated fraction) was calculated and used in bioleaching experiments as the maximum amount of phosphorus that could be

leached. The P_2O_5 content was 186,43 ± 34,1 mg/g in the 2nd fraction and 324,8 ± 26,19 mg/g in the concentrated fraction. ICP-MS analysis was performed (described in chapter 2.2.3.2.) to measure the content of metals in the solubilized concentrated phosphorite in three replicates. From REEs, the most represented elements were Y (482,1 ± 63,9 mg/kg), Ce (415,2 ± 38 mg/kg), Nd (211,5 ± 21,1 mg/kg) and La (207,1 ± 20,1 mg/kg) (Figure 9). The uranium content of the samples was 25,8 ± 2,2 mg/kg and vanadium content was 32,2 ± 8,4 mg/kg. The REEs and U content correspond well with what has been reported before in Estonian phosphorite (Graul *et al.*, 2023; Suomalainen, 2024).

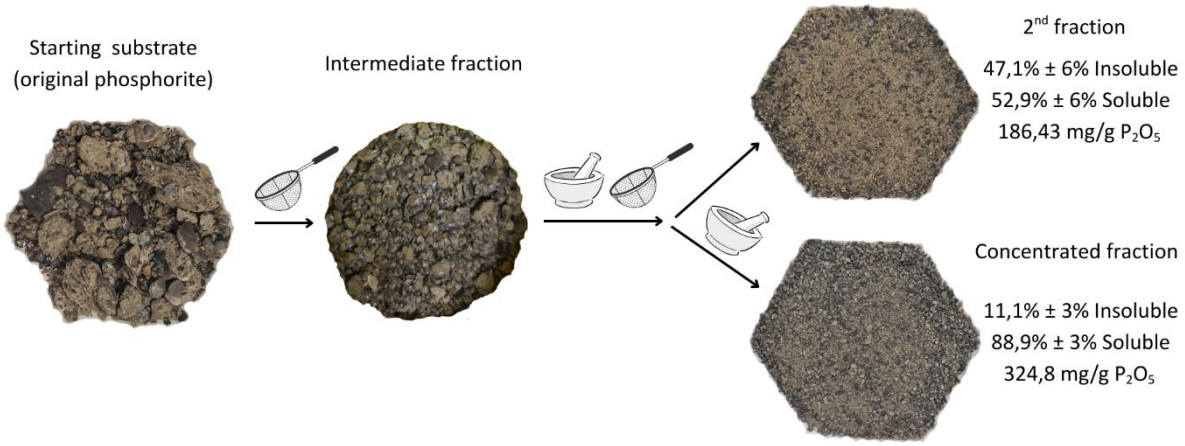

Figure 8. The change in composition of phosphorite after grinding and sieving. The 2nd fraction is removed after grinding the intermediate fraction. The concentrated fraction is ground once more to obtain finer particles. The variance is shown with the average's 95% confidence interval (CI).

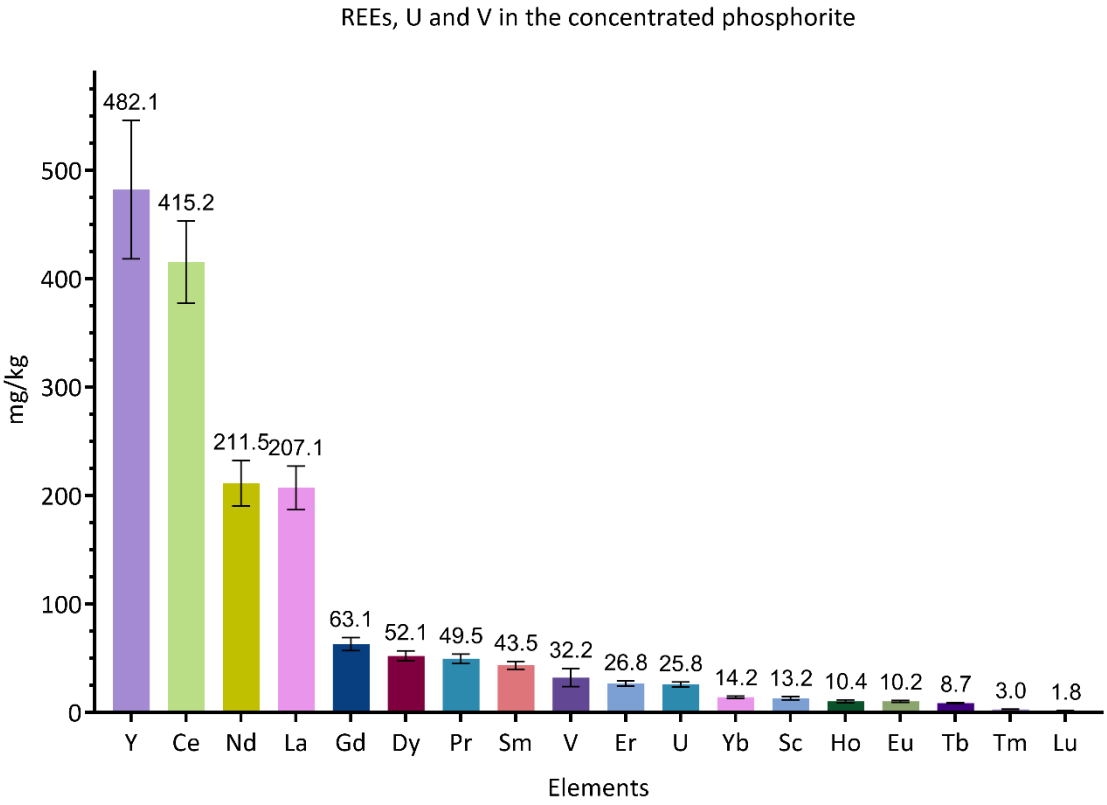

Figure 9. REEs, uranium (U) and vanadium (V) in the concentrated phosphorite. The amounts are shown as mg of the element per kg of the solubilized concentrated phosphorite. The concentrations were measured using ICP-MS (chapter 2.2.3.2.). The 95% confidence interval of the average is shown with error bars (n=3).

2.3.2. Sample collection test

To test for unintentional cell breakage during centrifugation, which could release intracellular phosphorus to the medium and thus raise the phosphorus levels, a comparison of sample collection methods was performed. It was determined that centrifuging the samples at 13000 rpm does not affect the phosphorus amount detected, compared to 5000 rpm and filtering (Figure 10). The samples were collected for each method in triplicate on days 1, 2, 3 and 4 of a bioleaching experiment. The solubilization percentages were calculated in comparison to the total phosphorus solubilized by acid digestion (324,8 mg/g). There was no statistically significant difference in the methods compared. Therefore, 13000 rpm centrifuging was used for sample preparation in the cases where the fungi agglomerated. When the fungi were dispersed in medium, the centrifuging step was changed to filtration through 0,22 µm syringe filter due to the difficulties in biomass sedimentation when centrifuging.

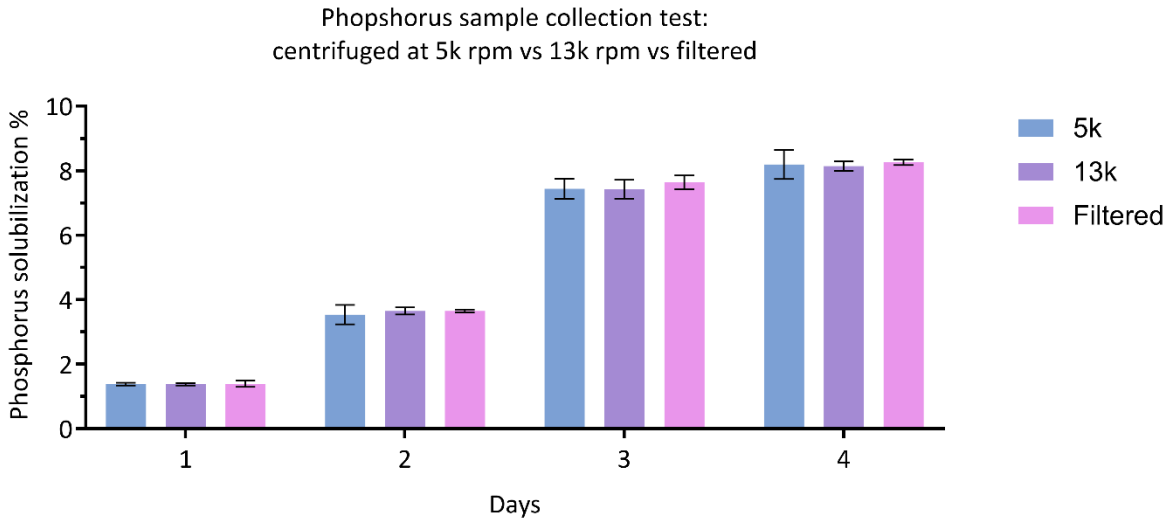

Figure 10. Results of the phosphorus sample collection test. Phosphorus content was measured spectrophotometrically (chapter 2.2.3.1.). The 95% confidence interval of the average is shown with error bars (n=3). Statistical analysis was performed using two-way analysis of variance (ANOVA) followed by Tukey's post hoc test for multiple comparisons. The value of $p < 0.05$ was considered significant, all comparisons were non-significant (significance is not shown on graph). P values are shown in Appendix 1.

2.3.3. Initial bioleaching experiment

Initial experiment with *A. japonicus* was done in 4 replicates, with 4 replicates of blank experiments (without inoculum) in parallel. The effect of the media on solubilization was low (0,75% ± 0,23% of P leached on day 28, data shown in Appendix 2). The blank values were subtracted from the results to only show the impact of *A. japonicus* on the solubilization of phosphorus (Figure 11). The culture was visually dispersed during the first two weeks, forming small spheres and swollen hyphal branches before one large agglomerate formation. By day 14, the fungi had agglomerated in 3 out of 4 replicates (Appendix 3).

Leaching of REEs was not detected (data not presented); however, uranium and vanadium were leached with a similar trend as phosphorus for the first 14 days (Figure 11). Uranium and vanadium solubilizations are likely strongly affected by pH, as the highest solubilizations (U - 16,7% ± 5,2%, V - 13,9% ± 5,2%) were reached on day 14 while the pH was lowest at around 3,5. The solubilized uranium and vanadium content plummeted after 14 days, coinciding with the pH rise in the lixiviant (Figure 11). By day 7, 14,9% ± 1,2% of phosphorus was leached, after which the solubilization plateaued with a 2% increase in the following 21 days (Figure 11). Similar phosphorus solubilization rates with the same organism and media were observed by Mahgoub *et al.*, 2022 and Xiao *et al.*, 2018 (Table 1).

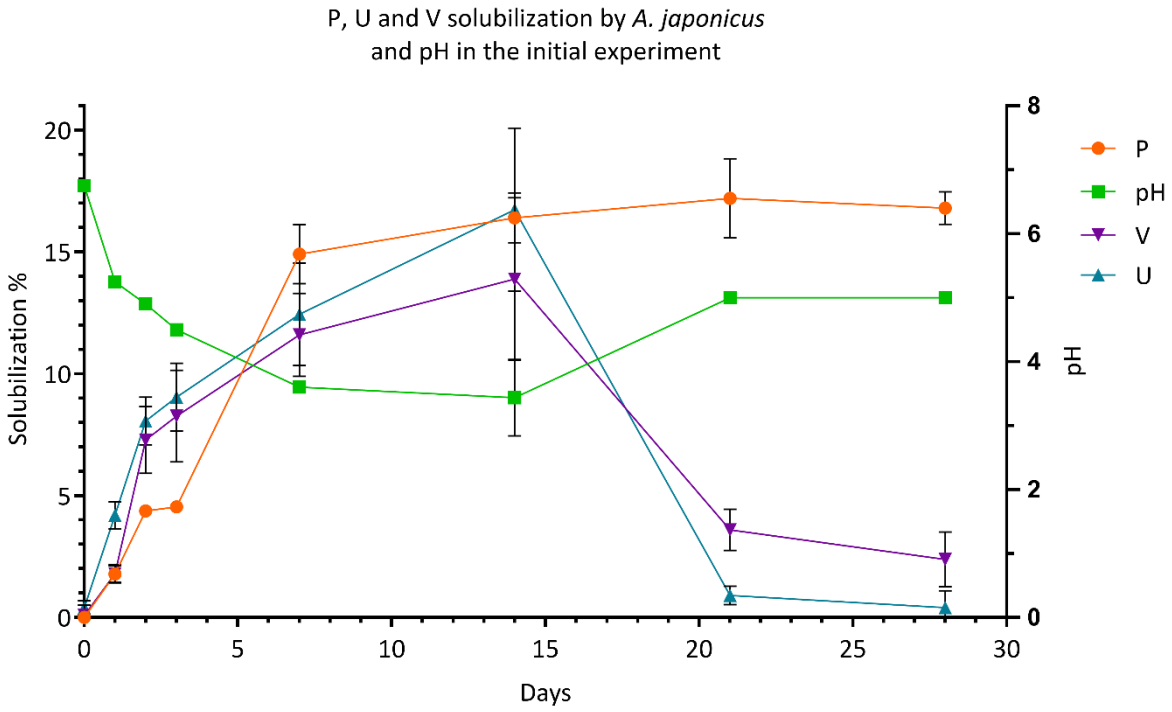

Figure 11. P, U and V solubilization by *A. japonicus* and pH in the initial experiment. Phosphorus content was measured spectrophotometrically (chapter 2.2.3.1.). Uranium and vanadium

concentrations were measured using ICP-MS (chapter 2.2.3.2.). The 95% confidence interval of the average is shown with error bars (n=4).

2.3.4. Leaching using different C/N ratios with NBRIP in batch culture

The main bioleaching mechanism by *A. japonicus* is believed to be associated with organic acid production and secretion (Mahgoub *et al.*, 2022; Xiao *et al.*, 2018). Therefore, increasing organic acid production would likely lead to an increased leaching efficiency. One way to elevate the production of organic acids is to increase the C/N ratio of the medium. A high C/N ratio typically favors the production of organic acids, such as citric acid and gluconic acid (discussed in chapter 1.2.2. Acidolysis) (Xiao *et al.*, 2018). However, out of the C/N ratios tested (50, 100, 146 and 200), the lowest C/N ratio produced the highest phosphorus solubilization results (Figure 12). This can be explained by nitrogen being more limiting than carbon, which can lead to lower biomass and, therefore, lower amounts of organic acids produced. A similar trend was observed with pH, the C/N=50 had the lowest pH while C/N=200 had the highest (Figure 13).

Blank experiments were done in 4 replicates for each condition. The leaching effect of the NBRIP medium reached 1% for all conditions on day 14 (data is shown in Appendix 2). The leaching effect of the medium is subtracted in the results shown in Figure 12. The average phosphate solubilizations on day 28 were 31,24% ± 0,46% (C/N=50); 24,72% ± 7,37 (C/N=100); 17,52% ± 1,22% (C/N=146) and 12,79% ± 1,03% (C/N=200). The phosphate solubilizations plateaued around day 7 until day 14, and after day 14 continued to increase for C/N ratios 50 and 100, while C/N ratios 146 and 200 remained plateaued until day 21 and in the last 7 days increased slightly (Figure 12). One replicate in the C/N=100 series had higher phosphorus solubilization than the other three replicates on days 21 and 28, which resulted in a wide 95% confidence interval of the average ± 5,7% and ± 7,4% respectively (Figure 12). The replicate was included in the results, as there was no clear indication (such as contamination) for exclusion.

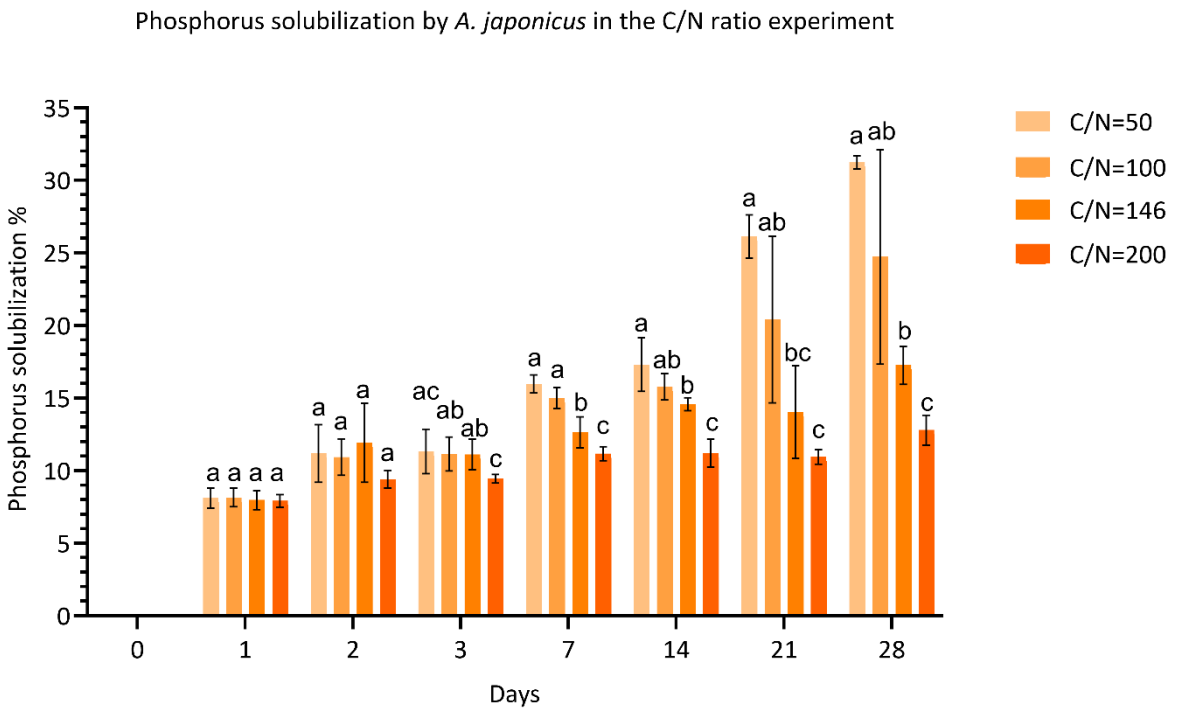

Figure 12. Phosphorus solubilization by *A. japonicus* in the C/N ratio experiment Phosphorus content was measured spectrophotometrically (chapter 2.2.3.1.). The 95% confidence interval of the average is shown with error bars (n=4). Statistical analysis was performed using two-way analysis of variance (ANOVA) followed by Tukey's post hoc test for multiple comparisons. The value of $p < 0.05$ was considered significant. Compact letter display is used to show significance on each day; non-significant groups share the same letter, while significantly different groups are allocated different letters. P-values are shown in Appendix 1.

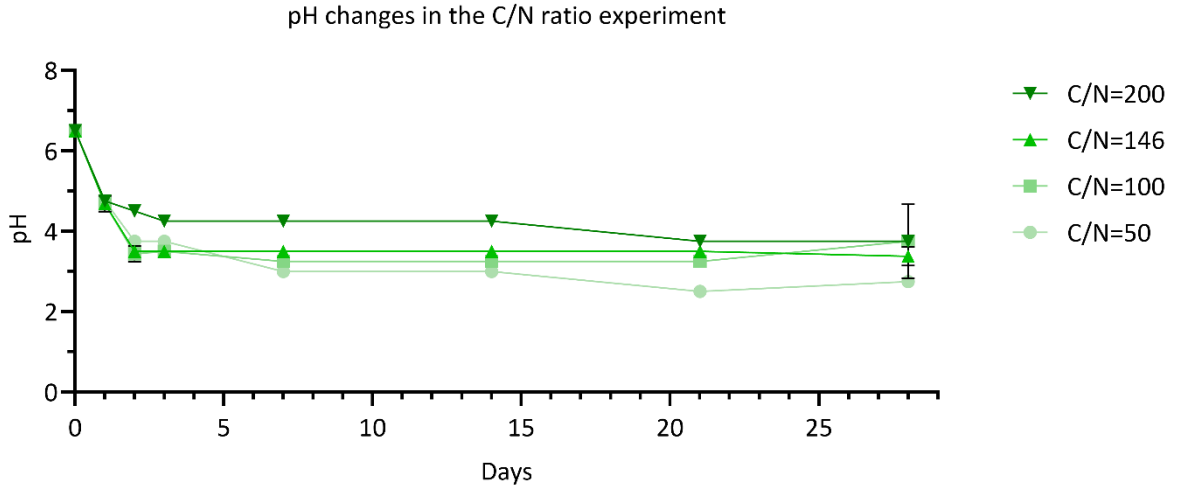

Figure 13. pH changes in the C/N ratio experiment. The 95% confidence interval of the average is shown with error bars (n=4).

A difference in the consistency of the biomass between the C/N ratio experiments was observed (Figure 14 and 15). All four of the C/N=50 experiments' biomass was in one agglomerate, while all four of the C/N=200 experiments were dispersed. The earliest agglomeration started for two replicates of C/N=50 experiments on day 3. A variance in the pH

was observed between the replicates of the C/N=100 and C/N=146 experiments on day 28, which may explain why two replicates for these conditions were dispersed and two agglomerated (Figures 13, 14 and 15). This C/N ratio is therefore believed to represent a "borderline" situation between two separate growing conditions. The pH dropped lower with lower C/N ratio values, which is likely tied to the differences in agglomeration, as pH is known to be the main parameter influencing fungal morphology (Zhang & Zhang, 2016). The lower C/N ratio might result in bigger biomass, which was not measured in our study, but could be explained by the higher amount of nitrogen available in the medium. Nitrogen limitation, with 1-2 g/L of $NaNO_3$ compared to 3 g/L, has been shown to significantly lower biomass and spore density in *Aspergillus oryzae* (Lv *et al.*, 2021). In our case $(NH_4)_2SO_4$ was used in concentrations of: 4,4 g/L for C/N=50; 2,2 g/L for C/N= 100; 1,5 g/L for C/N=146 and 1,1 g/L C/N=200. The C/N=50 medium can be considered nitrogen sufficient, and the rest have varying degrees of nitrogen limitation, which likely hinders biomass production. Bigger biomass, provided by nitrogen sufficiency, could lead to higher organic acid production due to the simple effect of there being more cells that produce and secrete acids.

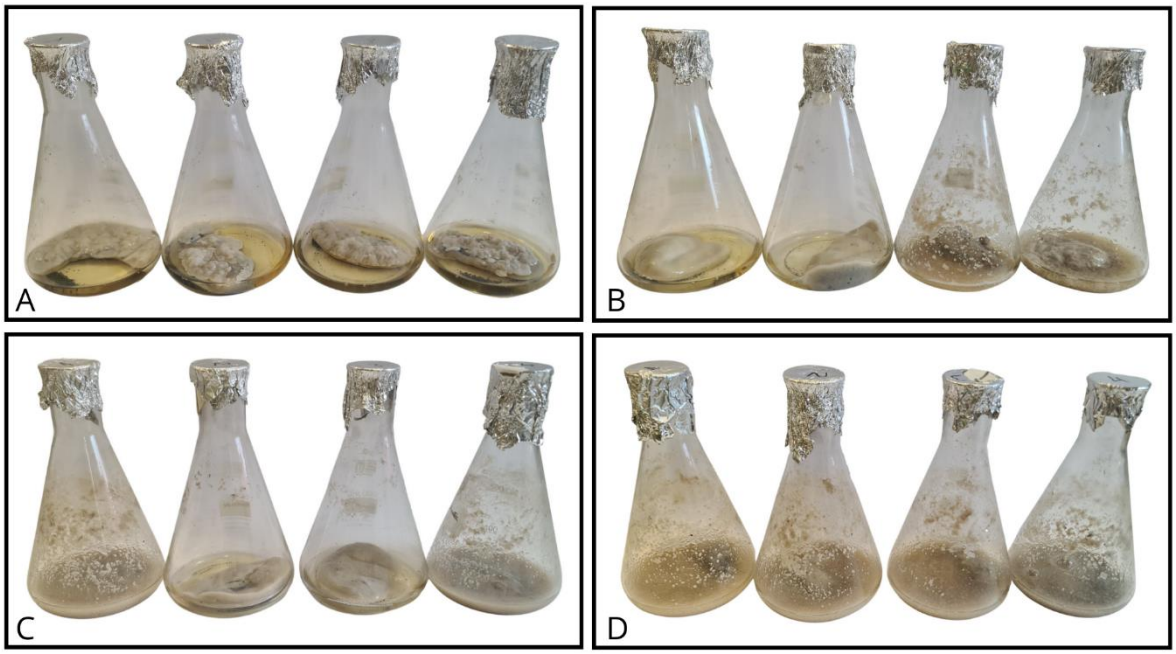

Figure 14. C/N ratio experiments on day 27. A. C/N=50, all 4 are in agglomerate B. C/N=100, 2 are in agglomerate, 2 are dispersed C. C/N=146, 2 are in agglomerate, 2 are dispersed D. C/N=200, all 4 are dispersed.

Figure 15. A close-up on the morphology of the fungi. On the left the fungi are completely agglomerated, while on the right the mycelia are dispersed throughout the medium.

ICP-MS analysis showed that no REEs leaching was detected (data not presented), but uranium (U) and vanadium (V) were leached (Figure 16 and 17). U leaching was rapid on the 1st day, however, the U leaching efficiency decreased in the following days, except for the C/N=200 condition, where it was 7,5% ± 1,3% on day 28. V was also leached at the highest rate on the 1st day, but contrary to U, the concentration continued to increase at a similar trend between the C/N ratios, like phosphorus (Figure 17). The C/N=50 had highest, C/N=100 average and C/N=146 and 200 had the lowest V solubilization. The final amount of V leached on day 28 was 23,3% ± 1,7 in C/N=50; 13% ± 13% in C/N=100; 6,9% ± 2,4% in C/N=146 and 8,3% ± 3,4% in C/N=200.

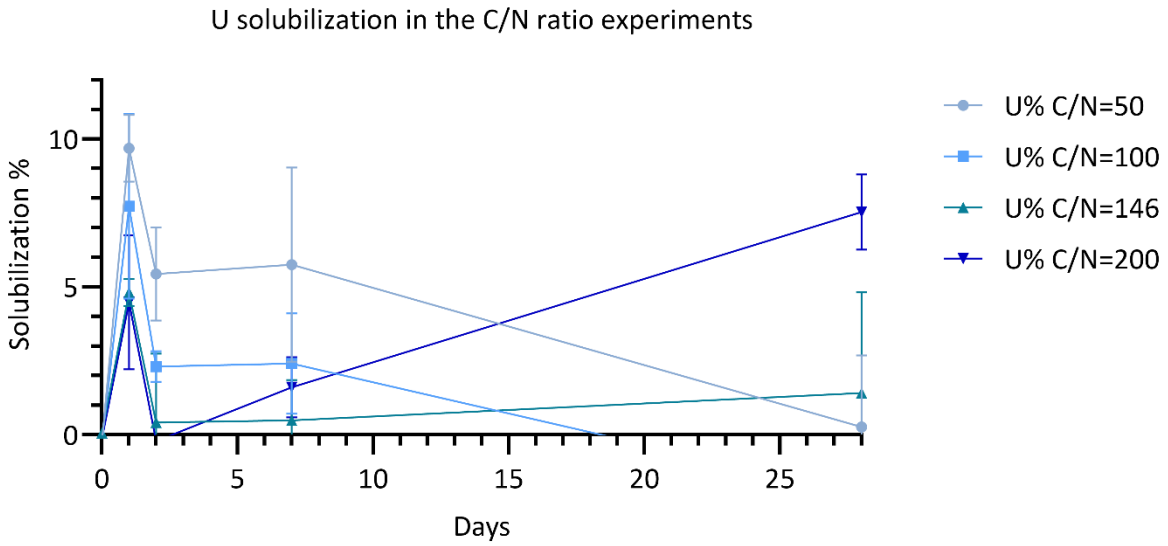

Figure 16. Uranium (U) solubilization in the C/N ratio experiment. The concentrations were measured using ICP-MS (chapter 2.2.3.2.). The 95% confidence interval of the average is shown with error bars (n=4).

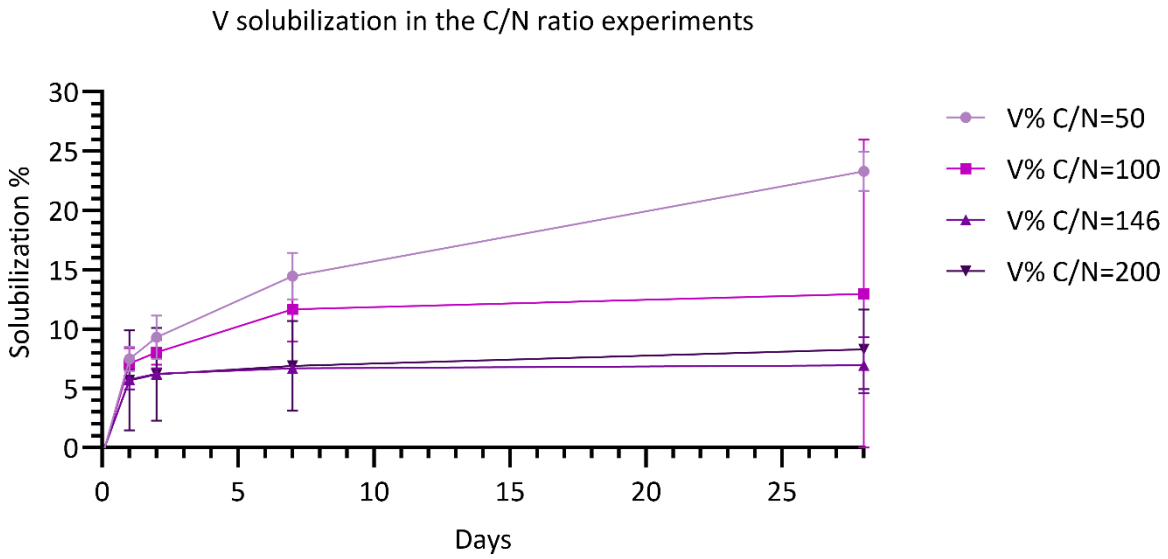

Figure 17. Vanadium (V) solubilization in the C/N ratio experiment. The concentrations were measured using ICP-MS (chapter 2.2.3.2.). The 95% confidence interval of the average is shown with error bars (n=4).

2.3.5. Leaching using C/N=200 NBRIP in semi-continuous setup

In the batch experiments, significant leaching took place in the first 48 hours. To extend the high leaching efficiency of the first 48 hours, a semi-continuous experiment was conducted, where fresh media was added after every 48 hours. The semi-continuous setup is a laboratory-scale equivalent to the packed-column and heap bioleaching. The semi-continuous culture in a shake flask is a preliminary step to column leaching, mimicking the flow of medium in the column, with the change of medium in the flask every 48 hours.

C/N ratio of 200 and 50, with 10% glucose in medium, were selected for the 48h semi-continuous bioleaching experiment to represent the spectrum of the C/N ratios tested in the previous experiment. For the first 2 days, there was no statistically significant difference in phosphorus solubilization in the batch experiments between the different C/N ratios (Figure 12), which is why C/N=200 was included in addition to the C/N=50, which showed the highest results. The 10% glucose in medium exhibited a steeper solubilization curve on the first days of the experiment than 1% glucose, which is why it was used for the semi-continuous experiment. In the initial experiment 1% glucose was used and P solubilization was nearly 5% on day 2, while the 10% glucose in the C/N ratio experiments provided a solubilization of over 10% on day 2 (Figure 11 and 12). Three replicates of blank experiments were done in parallel and subtracted from the results (Figure 18).

Samples for the phosphorus measurements were collected after every 24 hours. Every 48 hours the biomass and phosphorite were centrifuged, the lixiviant removed and fresh medium added. The phosphorus solubilization was calculated by adding the last cycle's solubilized phosphorus amount to the next. Phosphorus solubilization of 60,3% ± 0,4% was reached on day 30 (Figure 18). Secretion of organic acids decreased the pH in the freshly added medium during the cultivation cycle, resulting in up-and-down fluctuation during the sequential cycles (Figure 19). In the semi-continuous setup, the fungus has a high supply of glucose and ammonium sulphate (the C- and N-sources), because of the media change every 48h, which leads to biomass increase and faster acidification of the media.

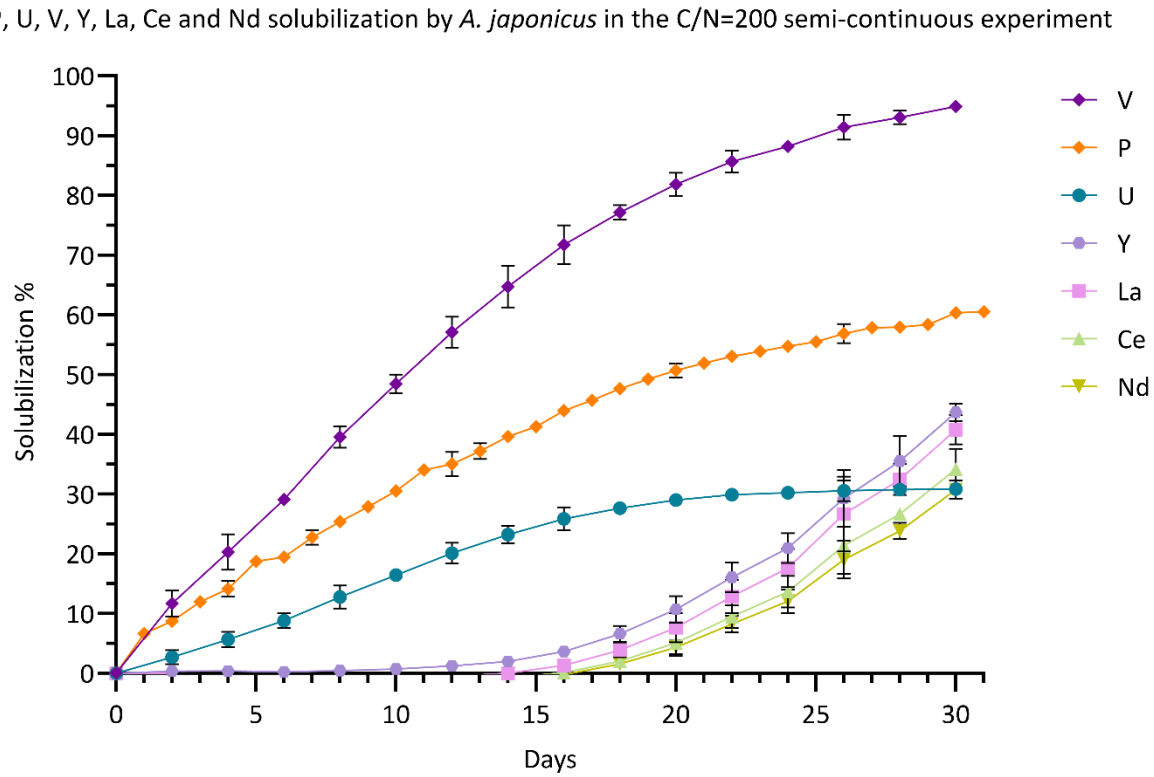

Figure 18. P, U, V, Y, La, Ce an Nd solubilization by *A. japonicus* in the C/N=200 semi-continuous experiment. Only the effect of *A. japonicus* is shown, blanks are subtracted. Phosphorus content was measured spectrophotometrically (chapter 2.2.3.1.). The U, La, Ce and Nd concentrations were measured using ICP-MS (chapter 2.2.3.2.). The 95% confidence interval of the average of each measurement is shown with error bars (n=3).

Uranium solubilization increased until day 22 to 30,9% ± 0,4% and then plateaued. The vanadium leaching was linear for the first 12 days with a 9-10% increase every 48h and then slowed down, with the final solubilization of 94,9 ± 0,4% on day 30. From REEs, yttrium (Y), lanthanum (La), cerium (Ce) and neodymium (Nd) started to leach around day 15. By day 30 43,7% ± 1,5% Y; 40,8% ± 2,5% La; 34,2% ± 3,4% Ce and 30,8% ± 1,5% Nd were leached, with leaching continuing on a linear slope (Figure 18). In the semi-continuous setup, the

phosphorite is dissolved more than in batch experiments. With the leachate removal every 48h, the fungus produces additional acids expressed in the lowering pH, which dissolves the material further.

In the semi-continuous experiments, REE solubilization seems to be influenced by competitive complexation dynamics, as the substrate contains a phosphorus concentration approximately 1000-fold greater than that of the REEs. Phosphorus is present at 324,8 ± 26,19 mg/g, while the REEs are 482,1 ± 63,9 mg/kg Y; 415,2 ± 38 mg/kg Ce; 211,5 ± 21,1 mg/kg Nd and 207,1 ± 20,1 mg/kg La. During the first two weeks of incubation, phosphorus is solubilized linearly, likely through the production of organic acids or siderophores by the fungus. This phase of bioleaching begins to slow down, eventually reaching a plateau, suggesting a depletion or reduced availability of bioaccessible phosphorus.

Interestingly, REE solubilization is negligible during the early phase and begins to increase significantly only after day 15, demonstrating a linear trend. This time-related difference between phosphorus and REE solubilization indicates a competitive complexation mechanism, where fungal metabolites preferentially bind and solubilize phosphorus due to its high abundance. As the availability of phosphorus decreases, these same metabolites seem to shift toward complexation with REEs, facilitating their subsequent leaching. This change in leaching behavior provides a practical advantage: lixiviant enriched in phosphorus can be collected during the early phase, while those with higher REE concentrations can be collected during the late phase. Therefore, without needing to purify phosphorus and REEs from the same mixture, extraction costs may be lower.

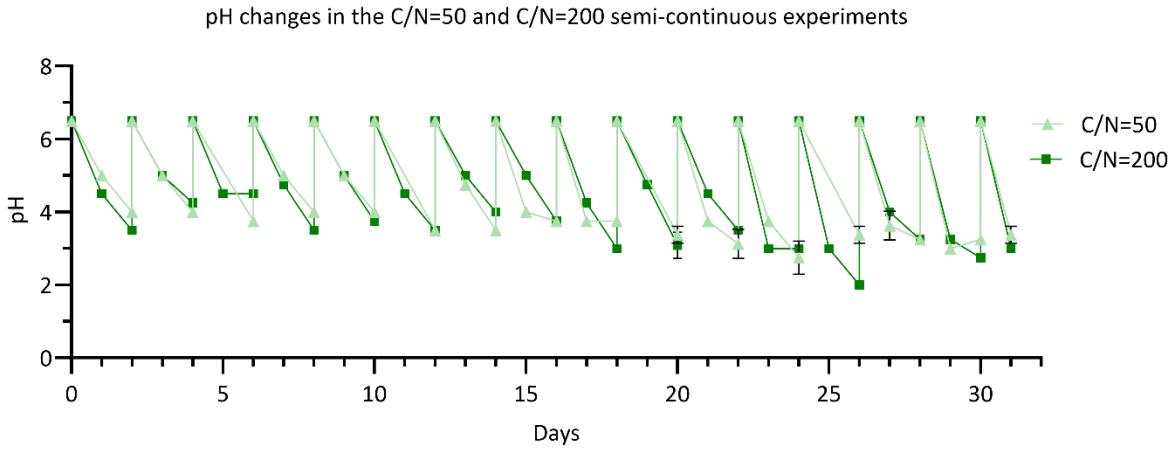

Figure 19. pH changes in the C/N=50 and C/N=200 semi-continuous experiments. C/N=200 condition is shown in dark green and C/N=50 light green. The 95% confidence interval of the average of each measurement is shown with error bars (n=3).

2.3.6. Leaching using C/N=50 NBRIP semi-continuous setup

C/N=50 was chosen for the semi-continuous experiment because it produced the best phosphorus solubilization in the batch experiments using different C/N ratios. Four replicates of blank experiments were conducted in parallel and were subtracted from the results (Figure 20). Samples were collected every 24 hours, while the medium was replaced every 48 hours, as in the semi-continuous C/N=200 experiment. The phosphorus solubilization reached 60% ten days earlier than in the C/N=200 experiment. The phosphorus solubilization plateaued at a similar value of around 60% for both semi-continuous conditions, indicating a limit to the amount that can be leached. The final phosphorus solubilization at the end of the experiment was 66,1% ± 0,6%. The pH changes were similar to the C/N=200 semi-continuous experiment (Figure 19).

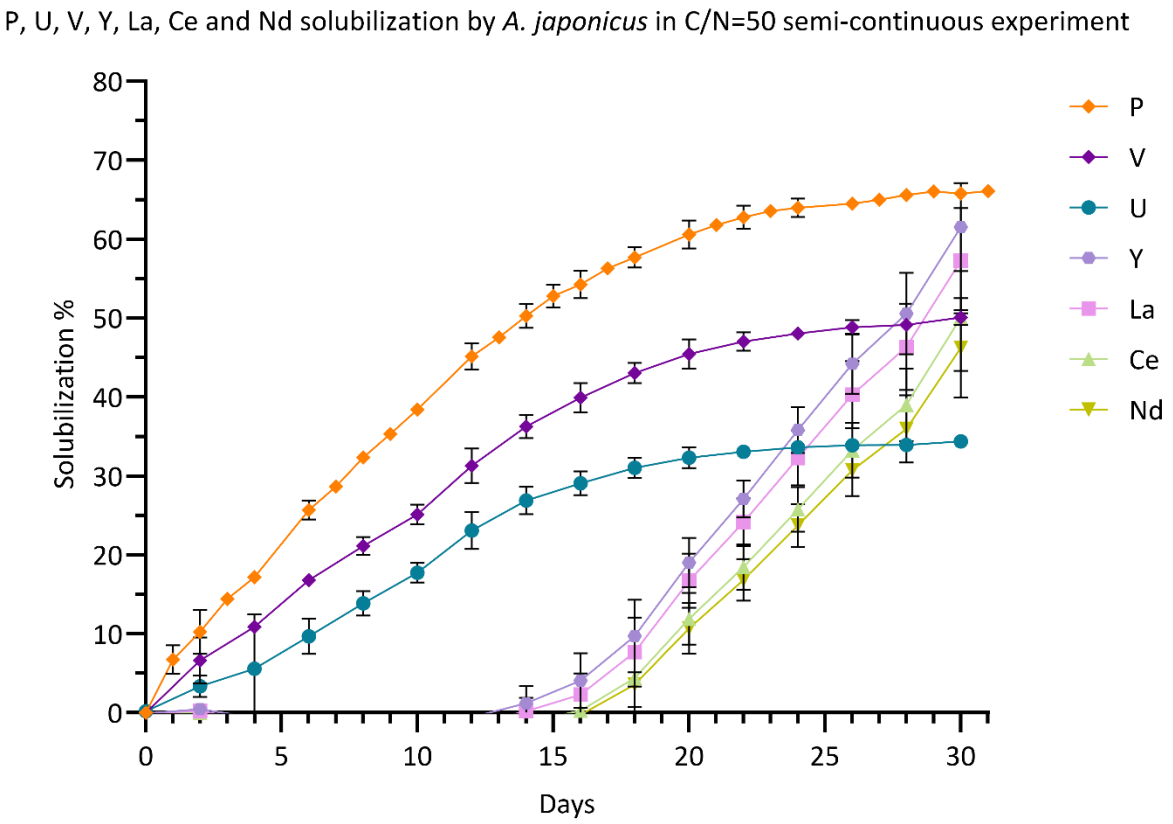

Figure 20. P, U, V, Y, La, Ce an Nd solubilization by *A. japonicus* in the C/N=50 semi-continuous experiment. Only the effect of *A. japonicus* is shown, blanks are subtracted. Phosphorus content was measured spectrophotometrically (chapter 2.2.3.1.). The U, La, Ce and Nd concentrations were measured using ICP-MS (chapter 2.2.3.2.). The 95% confidence interval of the average for each measurement is shown with error bars (n=4).

The uranium and REEs were leached in a similar trend to the C/N=200 experiment, although to a greater extent. By day 30, 34,4% ± 0,39% U; 61,5% ± 5,6% Y; 57,3% ± 6,7% La; 50,1% ± 6,8% Ce and 46,2% ± 6,3% Nd were leached (Figure 20). Uranium solubilization plateaued

around day 22 (33,1% ± 0,9% leached) and the REEs were still increasing at day 30. The REE solubilization, which started around the same time that P plateaued, is likely due to the same complexation mechanism, as described in the C/N=200 semi-continuous results chapter. Interestingly, vanadium was leached to a lower extent in the C/N=50 medium, at 50,1% ± 1% by day 30 compared to 94,9 ± 0,4% in the C/N=200 medium.

Phosphorus leaching efficiencies of 53,65% with pyrite and pH 8 have been reported using rock phosphate and *A. japonicus*. However, their report didn't include any absolute values of the phosphorus amounts (Table 1) (Singal *et al.*, 1994). The highest amount of phosphorus leached that has been reported in recent years using rock phosphate and *A. japonicus* is 35,3% on day 7 (Xiao *et al.*, 2018). In that study, 0,2% w/V of rock phosphate was used. The rock phosphate was ground to 100-200 mesh (Table 1). In our study, the greatest phosphorus solubilization was 66,1% in the semi-continuous setup on day 30, while using 1% w/V phosphorite, and the particle size was coarser. Finer particle size probably aids in the solubilization, as the fungus has more area on the material to attach to. In the future, grinding the phosphorite finer may be considered to raise leaching efficiencies. The 35,3% leaching efficiency achieved by Xiao *et al*. corresponds to 135 mg/L, our 66,1% corresponds to 2143,68 mg/L. Xiao *et al.* ran their experiments for 7 days, and the 135 mg/L was reported on the 7th day. The solubilization achieved in the semi-continuous experiment by 7th day was 28,7%, corresponding to 931,75 mg/L. The massive difference in amounts (mg/L) leached comes from several factors: 1) In our study, the medium was changed every 48 hours, providing fresh nutrients for the fungi 2) 10% glucose was used instead of 1% 3) The amount of substrate used was 5x higher.

The higher leaching efficiencies achieved by the lowest C/N ratio indicate that another mechanism may influence bioleaching results in addition to the production and secretion of organic acids. One possibility for this is the production of siderophores. *A. niger* has been found to produce a siderophore, which can extract REEs (Osman *et al.*, 2019). Therefore, it is plausible that a similar siderophore exists in *A. japonicus* as well. In fact a species from the same genus, *Aspergillus fumigatus*, is a model system for iron metabolism of siderophore-producing fungal species (Misslinger *et al.*, 2021). Iron limitation causes changes in gene expression in *Aspergilli*, resulting in increased siderophore biosynthesis (D. Odoni, 2017).

2.3.7. Organic acid measurements using assay kits

To clarify the participation of organic acids in bioleaching mechanisms of *A. japonicus*, it was planned to measure a series of acids highly produced by this fungus during the bioleaching procedure. Originally, organic acid concentrations were planned to be analyzed with high-performance liquid chromatography (HPLC). However, HPLC wasn't used in this study due to the absence of a suitable service in the University of Tartu and the high cost of ordering the analysis outside of the institute. Due to the time required for training and tuning the measurement conditions, the use of the institute's equipment was also unfeasible. Instead, colorimetric assay kits were purchased to measure the concentrations of α-ketoglutaric (Sigma-Aldrich), citric (Megazyme), gluconic (Megazyme) and tartaric acid (Megazyme) (Table 3). α-ketoglutaric acid measurement is based on an enzymatic reaction that results in hydrogen peroxide release and can be detected by peroxidase substrate at an absorbance of 570 nm. Citric acid measurement is based on the formation of oxaloacetate and acetate from citrate, catalyzed by citrate lyase. The consumption of NADH+ by the following enzymatic reactions (oxaloacetate conversion to pyruvate and pyruvate to D-lactate) is measured by the decrease in absorbance at 340 nm. D-gluconic acid quantification is based on the increase of NADPH concentration (stoichiometric to D-gluconic acid), formed during a 2-step reaction and measured at 340 nm. The measurement of gluconic acid and citric acid concentrations are based on the absorbance difference before and after colorimetric reaction. The principle of tartaric acid measurement is not detailed by the producer, but as in case of gluconic and citric acid kits, two measurements are taken at 505 nm and change in absorbance is proportional to the acid amount.

In case of citric, gluconic and tartaric acid, samples returned a high absorbance in initial measurements, exceeding the upper limit of the standard curve (absorbances are provided in Appendix 4). Additionally, while different dilutions were tested, the decrease or increase in absorbance (proportional to organic acid amount) did not correlate with the sample dilution factor. Therefore, it was caused not by an unexpectedly high organic acid concentration, but by an interfering compound and/or a non-specific reaction. In case of tartaric acid measurement, the samples' absorbances after colorimetric reaction were also out of range, being under the calibration curve. In case of α-ketoglutaric acid, the fresh NBRIP medium influenced the colorimetric reaction in the presence of α-ketoglutaric acid (Appendix 4). A blank measurement containing working solution and NBRIP, but no α-ketoglutaric acid,

provided similar or lower results than a blank prepared according to the protocol, with working solution and PBS (Appendix 4). Due to these inconsistencies, the results provided with these measuring kits are untrustworthy for *A. japonicus* cultures under these conditions, even if they are in the detectable range (summary and data provided in Table 3 and Appendix 4).

Table 3. Problems with the organic acid measurements. PBS – phosphate-buffered saline. A1 – absorbance before colorimetric reaction. Additional information can be found in Appendix 4.

Acid and reference code	Company	Wavelength	Detectable concentration	Problem
α-ketoglutaric (MAK541)	Sigma-Aldrich	570 nm	0,228-14,6 mg/L	Medium interference: standard with medium is 2-10x higher than standard with PBS
Citric (K-CITR)	Megazyme	340 nm	5-500 mg/L	Spent medium interference: high A1
Gluconic (K-GATE)	Megazyme	340 nm	80-500 mg/L	Spent medium interference: high A1
Tartaric (K-TART)	Megazyme	505 nm	150-11000 mg/L	Samples are under the calibration curve Spent medium interference: high A1

2.3.8. Future prospects

Results presented in here demonstrate that Estonian phosphorite can be bioleached with PSF *A. japonicus*. The next step in developing an economically feasible industrial technology would be column bioleaching, a lab-scale equivalent to heap bioleaching. Heap bioleaching is successfully used for the processing of black shist ore in our neighboring country, Finland, where Ni, Co and Zn are produced (Tanaka, 2017; Tuovinen *et al.*, 2018). Therefore, it is a plausible option and should be studied as a potential cheap and environmentally friendly method for phosphorite processing. Heap bioleaching operations are proven to have far lower operating expenses, for example copper has been profitably recovered from mining wastes that have been discarded by previous mining operations as being too low-grade (Natarajan, 2018; Tanaka, 2017).

The first step in modifying PSF-based technology for heaps would be the use of a laboratory-scale stacked column. It has a higher solid-to-liquid ratio than what can be achieved in shake flasks, therefore providing an even better understanding of leaching efficiencies in heap leaching. Additionally, it mimics the heterogeneity of the ore and microbial consortium that is present in large heaps. As part of it, the reliance of the mechanism on organic acids and/or siderophores needs to be determined, as it would allow for improving the specific mechanism and thus increase the leaching efficiency. Additionally, manganese and iron limitation can be tested, as they may increase leaching efficiencies. These experiments are important to explore an alternative method for the processing of phosphorite.

SUMMARY

This study aimed to optimize a medium for bioleaching phosphorite with *A. japonicus* and determine the leaching efficiency of phosphorus and metals and the organic acids produced.

The initial experiment, with the original NBRIP medium, 14,9% ± 1,2% of phosphorus was leached by day 7 and plateaued with a 2% increase in the following 21 days. Uranium (U) and vanadium (V) solubilizations are likely strongly affected by pH, as the highest solubilizations of 16,7% ± 5,2% U and 13,9% ± 5,2% V were reached on day 14 when the pH was lowest, consequently, the U and V content lowered with the rise in pH.

The average phosphate solubilizations in the C/N ratio experiments on day 28 were 31,24% ± 0,46% (C/N=50); 24,72% ± 7,37% (C/N=100); 17,52% ± 1,22% (C/N=146) and 12,79% ± 1,03% (C/N=200). The phosphate solubilizations plateaued around day 7 until day 14, and after day 14 continued to increase for C/N ratios 50 and 100, while C/N ratios 146 and 200 remained plateaued until day 21 and in the last 7 days increased slightly. Our findings show that *A. japonicus* could leach phosphorus from phosphorite most effectively in a modified NBRIP medium with 10% (w/V) glucose and a C/N ratio of 50. The solubilization of REEs was not detected in the C/N ratio experiments. However, vanadium leaching on day 28 was 23,3% ± 1,7% in C/N=50; 13% ± 13% in C/N=100; 6,9% ± 2,4% in C/N=146 and 8,3% ± 3,4% in C/N=200. Uranium was leached rapidly on the 1st day and then decreased to around 0-1% for all conditions, except for C/N=200, where it was 7,5% ± 1,3% on day 28.

Phosphorus solubilization of 60% was reached 10 days earlier in the C/N=50 semi-continuous experiment (on day 20) than in the C/N=200 semi-continuous experiment (on day 30). The C/N=50 experiments' phosphorus solubilization plateaued around day 20, with only 6% increase in the following 10 days (final solubilization 66,1% ± 0,6%). In the C/N=50 semi-continuous experiments by day 30: 34,4% ± 0,39% U; 50,1% ± 1% V; 61,5% ± 5,6% Y; 57,3% ± 6,7% La; 50,1% ± 6,8% Ce and 46,2% ± 6,3% Nd were leached. The C/N=200 semi-continuous setup also leached these elements; the leaching efficiency was around 4% lower for U and about 16-17% lower for the REEs mentioned. Vanadium was leached to a higher extent (94,9% ± 0,4%) in the C/N=200 medium.

Fosfori ja haruldaste muldmetallide bioleostamine Eesti fosforiidist *Aspergillus japonicus*'ega

Keity-Carol Topper

Resümee

Fosfor on kriitiline ressurss põllumajanduses väetistes ning haruldased muldmetallid (REEd) on olulised elemendid erinevates kõrgtehnoloogilistes seadmetes, näiteks elektriautodes, tuuleturbiinides, päikesepaneelides, fluorestseeruvates ja LED lambipirnides, kuid ka sõjalises tehnoloogias, näiteks radaritehnoloogias ja raketijuhtimissüsteemides. Fosforiidi kivim sisaldab 4-20% fosforit (P_2O_5 kujul) ning Eesti fosforiidis leidub ka olulisel määral mõningaid haruldasi muldmetalle (La, Ce, Y, Nd, Sm, Pr ja Gd). Traditsiooniliselt töödeldakse fosforiiti keemiliste meetoditega, mis võivad põhjustada keskkonnareostust, eriti toksiliste jäätmete ja vee saastamise osas. Bioleostamises seevastu kasutatakse mikroorganisme, nt. baktereid ja seeni, et looduslikult lagundada mineraale, vähendades oluliselt kahjulike kemikaalide vajadust. Lisaks võib bioleostamine madalate kulude tõttu olla majanduslikult otstarbekas ka madala kvaliteediga maakide puhul. Suuremahulise fosforiidi bioleostamismeetodina võiks kasutada kuhjaleostust (ingl. k. heap leaching). Kuhjaleostamises veetakse purustatud ja aglomeeritud maak leostusplatsile kuhjaks. Leostuslahust piserdatakse kuhjale ning see imbub läbi kivimi poorsuse ja kogutakse pärast äravoolu metalli eraldamiseks. Kuhjaleostamise laboratoorseks analoogiks on kolonnipõhine bioleostus, kus vertikaalne kolonn täidetakse purustatud maagiga ning leostuslahus imbub läbi kolonni. Väiksemahulisem meetod on poolpidev kultiveerimine loksutuskolvis, mida saab kasutada optimeerimiseks enne kolonnileostust.

Töö eesmärgiks oli optimeerida sööde fosforiidi bioleostamiseks *A. japonicus*ega. Söötme mõju organismi bioleostamise võimele hinnati peamiselt läbi fosfori leostumise efektiivsuse. Fosfori leostumist mõõdeti spektrofotomeetriliselt molübdovanadofosforhappena. Liksiviandist mõõdeti ka pH-d ning metallide ja uraani sisaldust ICP-MS meetodil. Bioleostumise mehhanismide paremaks mõistmiseks määrati erinevate söötmetega liksiviantidest järgmiste orgaaniliste hapete sisaldus: viinhape (tartaarhape), sidrunhape (tsitraat), glükoonhape ja α-ketoglutaraat. Katsetes kasutati NBRIP söödet, modifitseerides süsiniku (C) ja lämmastikuallika (N) koguseid, eesmärgiga leida optimaalne C/N suhte parima leostumiseffektiivsuse saavutamiseks.

Esialgses katses, algse NBRIP söötmega, leostus 7. päevaks 14,9% ± 1,2% fosforist ning püsis sellel tasemel vaid 2% suurenemisega järgmise 21 päeva jooksul. Uraani (U) ja vanaadiumi (V) lahustuvus on tõenäoliselt tugevalt mõjutatud pH-st, kuna lahustuvuse kõrgpunkt (16,7% ± 5,2% U ja 13,9% ± 5,2% V) saavutati 14. päeval, mil pH oli madalaim ning seejärel, pH tõustes, lahustuvused langesid.

Keskmine fosfori lahustuvus C/N suhte katsetes 28. päeval oli 31,24% ± 0,46% (C/N=50); 24,72% ± 7,37% (C/N=100); 17,52% ± 1,22% (C/N=146) ja 12,79% ± 1,03% (C/N=200). Fosfori lahustumine püsis stabiilsel tasemel umbes 7. päevast kuni 14. päevani. Pärast 14. päeva jätkus lahustuvuse tõus C/N suhete 50 ja 100 korral, samas kui C/N suhete 146 ja 200 korral jäid fosfori lahustuvused stabiilsele tasemele kuni 21. päevani ning viimase 7 päeva jooksul suurenesid veidi. Tulemused näitavad, et *A. japonicus* suutis fosforit fosforiidist kõige efektiivsemalt leostada modifitseeritud NBRIP söötmes, mis sisaldas 10% (w/V) glükoosi ja mille C/N suhe oli 50. REEde lahustumist C/N suhte katsetes ei tuvastatud. Vanaadiumi leostumine oli aga 28. päeval 23,3% ± 1,7% C/N=50 korral; 13% ± 13% C/N=100 korral; 6,9% ± 2,4% C/N=146 ja 8,3% ± 3,4% C/N=200 korral. Uraan leostus esimesel päeval kiiresti ja seejärel vähenes kõikide C/N suhete lõikes 0-1%-ni, välja arvatud C/N=200 söötmes, kus see oli 7,5% ± 1,3% 28. päeval.

Fosfori 60%-line lahustuvus saavutati C/N=50 poolpidevas katses 10 päeva varem (20. päeval) kui C/N=200 poolpidevas katses (30. päeval). C/N=50 katse fosfori lahustuvus saavutas platoo umbes 20. päeval, suurenedes järgmise 10 päeva jooksul vaid 6% võrra (lõplik lahustuvus 66,1% ± 0,6%). C/N=50 poolpidevas katses leostus 30. päevaks: 34,4% ± 0,39% uraani; 50,1% ± 1% vanaadiumi; 61,5% ± 5,6% üttriumi; 57,3% ± 6,7% lantaani; 50,1% ± 6,8% tseeriumi ja 46,2% ± 6,3% neodüümi. Samad elemendid leostusid ka C/N=200 poolpidevas katses, kuid leostumise efektiivsus oli umbes 4% madalam U ja 16-17% madalam REEde puhul. Vanaadiumi leostus C/N=200 söötmega katses rohkem, 30. päevaks oli leostunud 94,9% ± 0,4%.

REFERENCES

Abdel-Azeem, A. M., Abdel-Azeem, M. A., Abdul-Hadi, S. Y., & Darwish, A. G. (2019). Aspergillus: Biodiversity, Ecological Significances, and Industrial Applications. In A. N. Yadav, S. Mishra, S. Singh, & A. Gupta (Eds.), *Recent Advancement in White Biotechnology Through Fungi: Volume 1: Diversity and Enzymes Perspectives* (pp. 121–179). Springer International Publishing.

Alberts, B., Johnson, A., Lewis, J., Raff, M., Roberts, K., & Walter, P. (2002). *Molecular Biology of the Cell* (4th ed.). Garland Science.

Amiri, F., Mousavi, S. M., Yaghmaei, S., & Barati, M. (2012). Bioleaching kinetics of a spent refinery catalyst using *Aspergillus niger* at optimal conditions. *Biochemical Engineering Journal*, *67*, 208–217.

Beopoulos, A., Cescut, J., Haddouche, R., Uribelarrea, J.-L., Molina-Jouve, C., & Nicaud, J.-M. (2009). *Yarrowia lipolytica* as a model for bio-oil production. *Progress in Lipid Research*, *48*(6), 375–387.

Bleiwas, D. I. (2012). Estimated water requirements for gold heap-leach operations. In *Open-File Report* (Nos. 2012–1085). U.S. Geological Survey.

Brierley, C. L. (2001). Bacterial succession in bioheap leaching. *Hydrometallurgy*, *59*(2), 249–255.

Castro, L., Blázquez, M. L., González, F., Muñoz, J. A., & Ballester, A. (2017). Anaerobic bioleaching of jarosites by *Shewanella putrefaciens,* influence of chelators and biofilm formation. *Hydrometallurgy*, *168*, 56–63.

Cavallo, E., Charreau, H., Cerrutti, P., & Foresti, M. L. (2017). Yarrowia lipolytica: a model yeast for citric acid production. *FEMS Yeast Research*, *17*.

Christenson, E. A., & Schijf, J. (2011). Stability of YREE complexes with the trihydroxamate siderophore desferrioxamine B at seawater ionic strength. *Geochimica et Cosmochimica Acta*, *75*(22), 7047–7062.

Cocks, L. R. M., & Torsvik, T. H. (2005). Baltica from the late Precambrian to mid-Palaeozoic times: The gain and loss of a terrane's identity. *Earth-Science Reviews*, *72*(1), 39–66.

Dong, Y., Zan, J., & Lin, H. (2023). Bioleaching of heavy metals from metal tailings utilizing bacteria and fungi: Mechanisms, strengthen measures, and development prospect. *Journal of Environmental Management*, *344*, 118511.

Dronawat, S. N., Svihla, C. K., & Hanley, T. R. (1995). The effects of agitation and aeration on the production of gluconic acid byAspergillus niger. *Applied Biochemistry and Biotechnology*, *51*(1), 347–354.

Dusengemungu, L., Kasali, G., Gwanama, C., & Mubemba, B. (2021). Overview of fungal bioleaching of metals. *Environmental Advances*, *5*, 100083.

European Commission, E. (2024). *Agri-environmental indicator - mineral fertiliser consumption*. https://ec.europa.eu/eurostat/statistics-explained/index.php?title=Agri-environmental_indicator_-_mineral_fertiliser_consumption

Evans, C. T., & Ratledge, C. (1985). Possible regulatory roles of ATP:citrate lyase, malic enzyme, and AMP deaminase in lipid accumulation by Rhodosporidium toruloides CBS 14. *Canadian Journal of Microbiology*, *31*(11), 1000–1005.

Gericke, M., Neale, J., & van Staden, P. (2009). A Mintek perspective of the past 25 years in minerals bioleaching. *Journal- South African Institute of Mining and Metallurgy*, *109*, 567–585.

Goldberg, I., Rokem, J. S., & Pines, O. (2006). Organic acids: old metabolites, new themes. *Journal of Chemical Technology & Biotechnology*, *81*(10), 1601–1611.

Graul, S., Kallaste, T., Pajusaar, S., Urston, K., Gregor, A., Moilanen, M., Ndiaye, M., & Hints, R. (2023). REE + Y distribution in Tremadocian shelly phosphorites (Toolse, Estonia): Multi-stages enrichment in shallow marine sediments during early diagenesis. *Journal of Geochemical Exploration*, *254*, 107311.

Grewal, H. S., & Kalra, K. L. (1995). Fungal production of citric acid. *Biotechnology Advances*, *13*(2), 209–234.

Gu, S., Fu, B., & Ahn, J. W. (2020). Simultaneous Removal of Residual Sulfate and Heavy Metals from Spent Electrolyte of Lead-Acid Battery after Precipitation and Carbonation. *Sustainability*, *12*(3), Article 3.

Hathaway, J. A., & Atkinson, D. E. (1963). The Effect of Adenylic Acid on Yeast Nicotinamide Adenine Dinucleotide Isocitrate Dehydrogenase, a Possible Metabolic Control Mechanism. *Journal of Biological Chemistry*, *238*(8), 2875–2881.

Heikkinen, V., Arpalahti, A., & Garcia-Balbuena, D. (2022). Process Update on Dynamic Heap Bioleaching of a Black Schist Ore. *Proceedings of Heap Leach Solutions*.

Holah, Sh. Sh., Abou-Zeid, S. T., Taalab, A. S., Siam, H. S., & Abd El-Rahman, E. A. (2019). Effect of organic and mineral acids on release of phosphorus from phosphate rocks. *Middle East Journal of Agriculture Research*, *8*(3), 917–927.

Jones, S., & Santini, J. (2023). Mechanisms of bioleaching: iron and sulfur oxidation by acidophilic microorganisms. *Essays in Biochemistry*, *67*.

Jorjani, E., & Askari Sabzkoohi, H. (2022). Gold leaching from ores using biogenic lixiviants – A review. *Current Research in Biotechnology*, *4*, 10–20.

Khandelwal, R., Srivastava, P., & Bisaria, V. S. (2023). Recent advances in the production of malic acid by native fungi and engineered microbes. *World Journal of Microbiology and Biotechnology*, *39*(8), 217.

Knuf, C., Nookaew, I., Brown, S. H., McCulloch, M., Berry, A., & Nielsen, J. (2013). Investigation of Malic Acid Production in Aspergillus oryzae under Nitrogen Starvation Conditions. *Applied and Environmental Microbiology*, *79*(19), 6050–6058.

Kornberg, Arthur., & Pricer, W. E. (1951). DI- AND TRIPHOSPHOPYRIDINE NUCLEOTIDE ISOCITRIC DEHYDROGENASES IN YEAST. *Journal of Biological Chemistry*, *189*(1), 123–136.

Kundla, R. (2024, September 30). Lääne-Virumaal alustati fosforiidi testpuurimistega. *ERR*. https://www.err.ee/1609475496/laane-virumaal-alustati-fosforiidi-testpuurimistega

Ledesma-Amaro, R., & Nicaud, J.-M. (2016). *Yarrowia lipolytica* as a biotechnological chassis to produce usual and unusual fatty acids. *Progress in Lipid Research*, *61*, 40–50.

Li, H., Deng, Z., Oraby, E., & Eksteen, J. (2023). Amino acids as lixiviants for metals extraction from natural and secondary resources with emphasis on glycine: A literature review. *Hydrometallurgy*, *216*, 106008.

Li, S., Yang, J., Mohamed, H., Wang, X., Shi, W., Xue, F., López-García, S., Liu, Q., & Song, Y. (2024). AMP deaminase: A crucial regulator in nitrogen stress and lipid metabolism in *Mucor circinelloides*. *Biochimica et Biophysica Acta (BBA) - Molecular and Cell Biology of Lipids*, *1869*(2), 159434.

Liu, P., Wang, X., & Zhang, W. (2025). Impact of organic acids on extraction of rare earth elements: Mechanisms and optimization. *Journal of Rare Earths*.

Liu, R., Li, J., & Ge, Z. (2016). Review on *Chromobacterium Violaceum* for Gold Bioleaching from E-waste. *Procedia Environmental Sciences*, *31*, 947–953.

Lv, G., Xu, Y., Tu, Y., Cheng, X., Zeng, B., Huang, J., & He, B. (2021). Effects of Nitrogen and Phosphorus Limitation on Fatty Acid Contents in Aspergillus oryzae. *Frontiers in Microbiology*, *12*.

Mackey, K. R. M., & Paytan, A. (2009). Phosphorus Cycle. *Encyclopedia of Microbiology*, *3*, 322–334.

Mahgoub, S. A., Kedra, E. G. A., Abdelfattah, H. I., Abdelbasit, H. M., Alamoudi, S. A., Al-Quwaie, D. A., Selim, S., Alsharari, S. S., Saber, W. I. A., & El-Mekkawy, R. M. (2022). Bioconversion of Some Agro-Residues into Organic Acids by Cellulolytic Rock-Phosphate-Solubilizing Aspergillus japonicus. *Fermentation*, *8*(9), Article 9.

Malik, L., & Hedrich, S. (2022). Ferric Iron Reduction in Extreme Acidophiles. *Frontiers in Microbiology*, *12*.

Maneesuwannarat, S., Teamkao, P., Vangnai, A. S., Yamashita, M., & Thiravetyan, P. (2016). Possible mechanism of gallium bioleaching from gallium nitride (GAN) by *Arthrobacter creatinolyticus*: Role of amino acids/peptides/proteins bindings with gallium. *Process Safety and Environmental Protection*, *103*, 36–45.

Manesh, M. J. H., Willard, D. J., Lewis, A. M., & Kelly, R. M. (2024). Extremely thermoacidophilic archaea for metal bioleaching: *What do their genomes tell Us? Bioresource Technology*, *391*, 129988.

Michelsen, O. B. (1957). Photometric Determination of Phosphorus as Molybdovanadophosphoric Acid. *Analytical Chemistry*, *29*(1), 60–62.

Misslinger, M., Hortschansky, P., Brakhage, A. A., & Haas, H. (2021). Fungal iron homeostasis with a focus on *Aspergillus fumigatus*. *Biochimica et Biophysica Acta (BBA) - Molecular Cell Research*, *1868*(1), 118885.

Morin, D. H. R., & d'Hugues, P. (2007). Bioleaching of a Cobalt-Containing Pyrite in Stirred Reactors: a Case Study from Laboratory Scale to Industrial Application. In D. E. Rawlings & D. B. Johnson (Eds.), *Biomining* (pp. 35–55). Springer.

Natarajan, K. A. (2018). Chapter 5 - Methods in Biohydrometallurgy and Developments: Dump, Heap, In Situ, and Stirred Tank Bioleaching. In K. A. Natarajan (Ed.), *Biotechnology of Metals* (pp. 81–106). Elsevier.

Nautiyal, C. S. (1999). An efficient microbiological growth medium for screening phosphate solubilizing microorganisms. *FEMS Microbiology Letters*, *170*(1), 265–270.

NCBI. (2018). *Aspergillus japonicus genome assembly GCF_003184785.1 (ASM318478v1)* [dataset]. National Center for Biotechnology Information. https://www.ncbi.nlm.nih.gov/datasets/genome/GCF_003184785.1/

Neilands, J. B. (1995). Siderophores: Structure and Function of Microbial Iron Transport Compounds (*). *Journal of Biological Chemistry*, *270*(45), 26723–26726.

Ochsenreither, K., Fischer, C., Neumann, A., & Syldatk, C. (2014). Process characterization and influence of alternative carbon sources and carbon-to-nitrogen ratio on organic acid production by Aspergillus oryzae DSM1863. *Applied Microbiology and Biotechnology*, *98*(12), 5449–5460.

Odoni, D. (2017). *Organic acid production in Aspergillus niger and other filamentous fungi* [Doctor]. Wageningen Univesity & Research.

Odoni, D. I., van Gaal, M. P., Schonewille, T., Tamayo-Ramos, J. A., Martins dos Santos, V. A. P., Suarez-Diez, M., & Schaap, P. J. (2017). Aspergillus niger Secretes Citrate to Increase Iron Bioavailability. *Frontiers in Microbiology*, *8*, 1424.

Osman, Y., Gebreil, A., Mowafy, A. M., Anan, T. I., & Hamed, S. M. (2019). Characterization of Aspergillus niger siderophore that mediates bioleaching of rare earth elements from phosphorites. *World Journal of Microbiology and Biotechnology*, *35*(6), 93.

Pradhan, N., Nathsarma, K. C., Srinivasa Rao, K., Sukla, L. B., & Mishra, B. K. (2008). Heap bioleaching of chalcopyrite: A review. *Minerals Engineering*, *21*(5), 355–365.

Puhakka, J., & Tuovinen, O. H. (1986). Microbiological leaching of sulfide minerals with different percolation regimes. *Applied Microbiology and Biotechnology*, *24*, 144–148.

Raukas, A., & Teedumäe, A. (1997). *Geology and Mineral Resources of Estonia*. Estonian Academy Publishers. https://web.archive.org/web/20071211132438/http://sarv.gi.ee/geology/text.html#_Toc174709526

Ren, W.-X., Li, P.-J., Geng, Y., & Li, X.-J. (2009). Biological leaching of heavy metals from a contaminated soil by *Aspergillus niger*. *Journal of Hazardous Materials*, *167*(1), 164–169.

Riekkola-Vanhanen, M. (2013). Talvivaara mining company – From a project to a mine. *Minerals Engineering*, *48*, 2–9.

Saito, K. (1906). Untersuchungen tiber die atmosphaerischen Pilzkeime, I. *The Botanical Magazine Published by the Tokyo Botanical Society.*, *XX*, 61–63.

Saluorg, J. (2023). Teadlane: fosforiidi kaevandamisest rääkimine on ennatlik. *Novaator*.

Sankpal, N. V., & Kulkarni, B. D. (2002). Optimization of fermentation conditions for gluconic acid production using *Aspergillus niger* immobilized on cellulose microfibrils. *Process Biochemistry*, *37*(12), 1343–1350.

Saxena, J., Basu, P., Jaligam, V., Ch, S., & ra. (2013). Phosphate solubilization by a few fungal strains belonging to the genera Aspergillus and Penicillium. *African Journal of Microbiology Research*, *7*(41), 4862–4869.

Schoch, C. L., Ciufo, S., Domrachev, M., Hotton, C. L., Kannan, S., Khovanskaya, R., Leipe, D., Mcveigh, R., O'Neill, K., Robbertse, B., Sharma, S., Soussov, V., Sullivan, J. P., Sun, L., Turner, S., & Karsch-Mizrachi, I. (2020). NCBI Taxonomy: a comprehensive update on curation, resources and tools. *Database: The Journal of Biological Databases and Curation*, *2020*, baaa062.

Sengul, H., Ozer, A. K., & Gulaboglu, M. S. (2006). Beneficiation of Mardin-Mazıdağı (Turkey) calcareous phosphate rock using dilute acetic acid solutions. *Chemical Engineering Journal*, *122*(3), 135–140.

Seshadri, S., Ignacimuthu, S., & Lakshminarasimhan, C. (2004). Effect of nitrogen and carbon sources on the inorganic phosphate solubilization by different Aspergillus niger strains. *Chemical Engineering Communications*, *191*(8), 1043–1052.

Shi, X., Zeng, A., Duan, H., Zhang, H., & Yang, J. (2024). Status and development trends of phosphogypsum utilization in China. *Circular Economy*, *3*(4), 100116.

Singal, R., Gupta, R., & Saxena, R. K. (1994). Rock Phosphate Solubilization under Alkaline Conditions by Aspergillus japonicus and A. foetidus. *Folia Microbiologica*, *39*, 33–36.

Soesoo, A., Vind, J., & Hade, S. (2020). Uranium and Thorium Resources of Estonia. *Minerals*, *10*(9), Article 9.

Srichandan, H., Mohapatra, R. K., Parhi, P. K., & Mishra, S. (2019). Bioleaching approach for extraction of metal values from secondary solid wastes: A critical review. *Hydrometallurgy*, *189*, 105122.

Srichandan, H., Mohapatra, R. K., Singh, P. K., Mishra, S., Parhi, P. K., & Naik, K. (2020). Column bioleaching applications, process development, mechanism, parametric effect and modelling: A review. *Journal of Industrial and Engineering Chemistry*, *90*, 1–16.

Steenwyk, J. L., Balamurugan, C., Raja, H. A., Gonçalves, C., Li, N., Martin, F., Berman, J., Oberlies, N. H., Gibbons, J. G., Goldman, G. H., Geiser, D. M., Houbraken, J., Hibbett, D. S., & Rokas, A. (2024). Phylogenomics reveals extensive misidentification of fungal strains from the genus Aspergillus. *Microbiology Spectrum*, *12*(4), e03980-23.

Strasser, H., Burgstaller, W., & Schinner, F. (1994). High-yield production of oxalic acid for metal leaching processes by *Aspergillus niger*. *FEMS Microbiology Letters*, *119*(3), 365–370. https://www.sciencedirect.com/science/article/pii/0378109794904413

Suomalainen, H. O. (2024). *Distribution of Rare Earth Elements in Estonian Lower Ordovician Complexes [Magistritöö. Juhendaja: R. Hints; kaasjuhendaja S. Graul]*. https://kirjandus.geoloogia.info/reference/49609

Tanaka M. (2017). A Comparison Study of Heap Bioleaching Sites in Chile and Finland for Further Development of Biotechnology for Mining. *EVERGREEN Joint Journal of Novel Carbon Resource Sciences & Green Asia Strategy*, *4*(4), 1–7. https://hdl.handle.net/2324/1929724

Telfer, T. J., Richardson-Sanchez, T., Gotsbacher, M. P., Nolan, K. P., Tieu, W., & Codd, R. (2019). Analogues of desferrioxamine B (DFOB) with new properties and new functions generated using precursor-directed biosynthesis. *BioMetals*, *32*(3), 395–408.

Tian, J., Peng, X., Li, X., Feng, H., Jiang, Z., & Wei, Y. (2014). Phosphate Solubilizing Abilities of Two Fungi and their Potential for Promoting Zenia insignis Growth in Heavy Metal Contaminated Soil. *Journal of Pure and Applied Microbiology*, *8*(5), 3439–3449. https://microbiologyjournal.org/phosphate-solubilizing-abilities-of-two-fungi-and-their-potential-for-promoting-zenia-insignis-growth-in-heavy-metal-contaminated-soil/

Tuomela, P., Törmänen, T., & Michaux, S. (2021). *Strategic roadmap for the development of Finnish battery mineral resources*. Geological Survey of Finland.

Tuovinen, H., Pelkonen, M., Lempinen, J., Pohjolainen, E., Read, D., Solatie, D., & Lehto, J. (2018). Behaviour of Metals during Bioheap Leaching at the Talvivaara Mine, Finland. *Geosciences*, *8*(2), Article 2.

van Aswegen, P. C., van Niekerk, J., & Olivier, W. (2007). The BIOX™ Process for the Treatment of Refractory Gold Concentrates. In D. E. Rawlings & D. B. Johnson (Eds.), *Biomining* (pp. 1–33). Springer.

Veiter, L., Rajamanickam, V., & Herwig, C. (2018). The filamentous fungal pellet-relationship between morphology and productivity. *Applied Microbiology and Biotechnology*, *102*(7), 2997–3006.

Vera, M., Schippers, A., Hedrich, S., & Sand, W. (2022). Progress in bioleaching: fundamentals and mechanisms of microbial metal sulfide oxidation – part A. *Applied Microbiology and Biotechnology*, *106*(21), 6933–6952.

Wang, M., Li, J., Liu, H., Huang, S., Liu, X., Liu, Y., Awais, M., & Wang, J. (2025). Rare Earth Element Extraction from Ionic Rare Earth Ores by Two Typical Acidogenic Microorganisms, Aspergillus niger and Acidithiobacillus ferrooxidans. *International Journal of Molecular Sciences*, *26*(5), 1986.

Wen, Y., Liu, P., Wang, Q., Zhao, S., & Tang, Y. (2024). Organic Ligand-Mediated Dissolution and Fractionation of Rare-Earth Elements (REEs) from Carbonate and Phosphate Minerals. *ACS Earth and Space Chemistry*, *8*(5), 1048–1061.

Wu, S., Wang, L., Zhao, L., Zhang, P., El-Shall, H., Moudgil, B., Huang, X., & Zhang, L. (2018). Recovery of rare earth elements from phosphate rock by hydrometallurgical processes – A critical review. *Chemical Engineering Journal*, *335*, 774–800.

Wu, Y., Xu, Q.-H., Chen, Z.-L., Yang, L.-H., & Guo, D.-S. (2025). Synthetic biology meets Aspergillus: engineering strategies for next-generation organic acid production. *World Journal of Microbiology and Biotechnology*, *41*(2), 36.

Xia, L., Uribe, P., Liu, X., Yu, C., Chai, L., Liu, J., Qiu, W., & Qiu, G. (2013). Comparison of chalcopyrite bioleaching after different microbial enrichment in shake flasks. *World Journal of Microbiology and Biotechnology*, *29*(2), 275–280.

Xiao, C., Chi, R., Li, X., Xia, M., & Xia, Z. (2011). Biosolubilization of Rock Phosphate by Three Stress-Tolerant Fungal Strains. *Applied Biochemistry and Biotechnology*, *165*(2), 719–727.

Xiao, C., Tingting, L., Guang, X., & Ruan, C. (2018). Characteristics and Mechanisms of Biosolubilization of Rock Phosphate by Aspergillus japonicus. *Brazilian Archives of Biology and Technology*, *60*.

Xiqiang, L., Hui, Z., Yong, T., & Yunlong, L. (2020). REE Geochemical Characteristic of Apatite: Implications for Ore Genesis of the Zhijin Phosphorite. *Minerals*, *10*(11), Article 11.

Yin, X., Shin, H., Li, J., Du, G., Liu, L., & Chen, J. (2017). Comparative genomics and transcriptome analysis of Aspergillus niger and metabolic engineering for citrate production. *Scientific Reports*, *7*(1), 41040.

Yle. (2015, January 23). Talvivaara to seek new state bailout. *Yle*. https://yle.fi/a/3-7755344

Yokoyama, K., Wang, L., Miyaji, M., & Nishimura, K. (2001). Identification, classification and phylogeny of the Aspergillus section Nigri inferred from mitochondrial cytochrome b gene. *FEMS Microbiology Letters*, *200*(2), 241–246.

Zhang, J., & Zhang, J. (2016). The filamentous fungal pellet and forces driving its formation. *Critical Reviews in Biotechnology*, *36*(6), 1066–1077.

Zheng, X., Du, P., Gao, K., Du, Y., Cairns, T. C., Ni, X., Chen, M., Zhao, W., Ma, X., Yang, H., Zheng, P., & Sun, J. (2023). Genome-wide transcription landscape of citric acid producing Aspergillus niger in response to glucose gradient. *Frontiers in Bioengineering and Biotechnology*, *11*, 1282314.

WEBPAGES

Copper Development Association. (2004, May). *Producing copper nature's way: Bioleaching*. Innovations. Retrieved May 7, 2025, from https://copper.org/publications/newsletters/innovations/2004/05/producing_copper_natures_way_bioleaching.php

European Commission, Eurostat. (2024). *Agri-environmental indicator - mineral fertiliser consumption.* Statistics Explained. Retrieved May 7, 2025, from https://ec.europa.eu/eurostat/statistics-explained/index.php?title=Agri-environmental_indicator_-_mineral_fertiliser_consumption

Megazyme. (n.d.). *Enzymatic bioanalysis assay kits. https://www.megazyme.com/citric-acid-assay-kit?sSearch=citric%20a; https://www.megazyme.com/d-gluconic-acid-d-glucono-delta-lactone?sSearch=gluconic;* https://www.megazyme.com/tartaric-acid-assay-kit?sSearch=tartaric

Ministry of Economic Affairs and Employment of Finland. (2024). *Terrafamen uraanin talteenotto.* Retrieved May 7, 2025, from https://tem.fi/terrafamen-uraanin-talteenotto

Sigma-Aldrich. (n.d.). *α-Ketoglutaric acid assay kit (MAK054).* https://www.sigmaaldrich.com/EE/en/product/sigma/mak541

APPENDICES

APPENDIX 1. P-values.

Table A1. P-values from the phosphorus sample collection test. Statistical analysis was performed using two-way analysis of variance (ANOVA) followed by Tukey's post hoc test for multiple comparisons. The value of $p < 0.05$ was considered significant, all comparisons were non-significant (ns).

Day	Comparison	P-value	Interpretation
1	5k vs. 13k	0,9305	ns
	5k vs. Filtered	0,9135	ns
	13k vs. Filtered	0,8237	ns
2	5k vs. 13k	0,4011	ns
	5k vs. Filtered	0,3967	ns
	13k vs. Filtered	>0,9999	ns
3	5k vs. 13k	0,9948	ns
	5k vs. Filtered	0,181	ns
	13k vs. Filtered	0,1411	ns
4	5k vs. 13k	0,9051	ns
	5k vs. Filtered	0,8161	ns
	13k vs. Filtered	0,1161	ns

Table A2. P-values from the C/N ratio experiment. Statistical analysis was performed using two-way analysis of variance (ANOVA) followed by Tukey's post hoc test for multiple comparisons. The value of $p < 0.05$ was considered significant. Ns – non significant. * - significant.

Day	Comparison	P-value	Interpretation
1	C/N=50 vs. C/N=100	0,9983	ns
	C/N=50 vs. C/N=146	0,9692	ns
	C/N=50 vs. C/N=200	0,883	ns
	C/N=100 vs. C/N=146	0,9216	ns
	C/N=100 vs. C/N=200	0,7775	ns
	C/N=146 vs. C/N=200	0,996	ns
2	C/N=50 vs. C/N=100	0,9836	ns
	C/N=50 vs. C/N=146	0,8944	ns
	C/N=50 vs. C/N=200	0,1725	ns
	C/N=100 vs. C/N=146	0,73	ns
	C/N=100 vs. C/N=200	0,073	ns
	C/N=146 vs. C/N=200	0,164	ns
3	C/N=50 vs. C/N=100	0,9912	ns
	C/N=50 vs. C/N=146	0,983	ns
	C/N=50 vs. C/N=200	0,0799	ns
	C/N=100 vs. C/N=146	0,9999	ns
	C/N=100 vs. C/N=200	0,0482	*
	C/N=146 vs. C/N=200	0,0356	*

APPENDIX 1. continues

7	C/N=50 vs. C/N=100	0,066	ns
	C/N=50 vs. C/N=146	0,0016	*
	C/N=50 vs. C/N=200	<0,0001	*
	C/N=100 vs. C/N=146	0,0065	*
	C/N=100 vs. C/N=200	<0,0001	*
	C/N=146 vs. C/N=200	0,0485	*
14	C/N=50 vs. C/N=100	0,2164	ns
	C/N=50 vs. C/N=146	0,0476	*
	C/N=50 vs. C/N=200	0,0015	*
	C/N=100 vs. C/N=146	0,0568	ns
	C/N=100 vs. C/N=200	0,0001	*
	C/N=146 vs. C/N=200	0,0015	*
21	C/N=50 vs. C/N=100	0,1359	ns
	C/N=50 vs. C/N=146	0,001	*
	C/N=50 vs. C/N=200	<0,0001	*
	C/N=100 vs. C/N=146	0,0987	ns
	C/N=100 vs. C/N=200	0,0391	*
	C/N=146 vs. C/N=200	0,1477	ns
28	C/N=50 vs. C/N=100	0,1844	ns
	C/N=50 vs. C/N=146	<0,0001	*
	C/N=50 vs. C/N=200	<0,0001	*
	C/N=100 vs. C/N=146	0,1336	ns
	C/N=100 vs. C/N=200	0,04	*
	C/N=146 vs. C/N=200	0,0007	*

APPENDIX 2. Phosphorus solubilization by blanks.

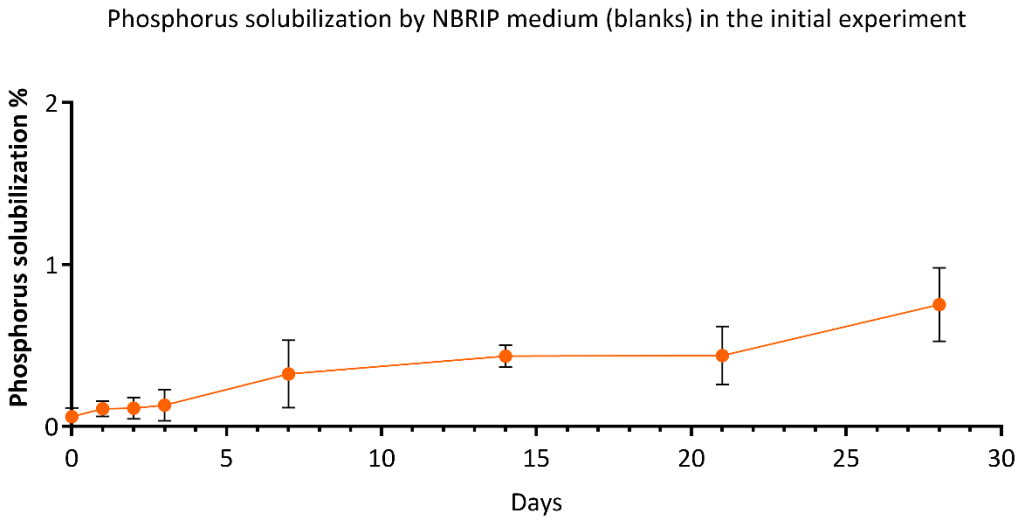

Figure A1. Phosphorus solubilization by 1% glucose NBRIP medium (blank) in the initial experiment. The 95% confidence interval of the average is shown with error bars (n=4).

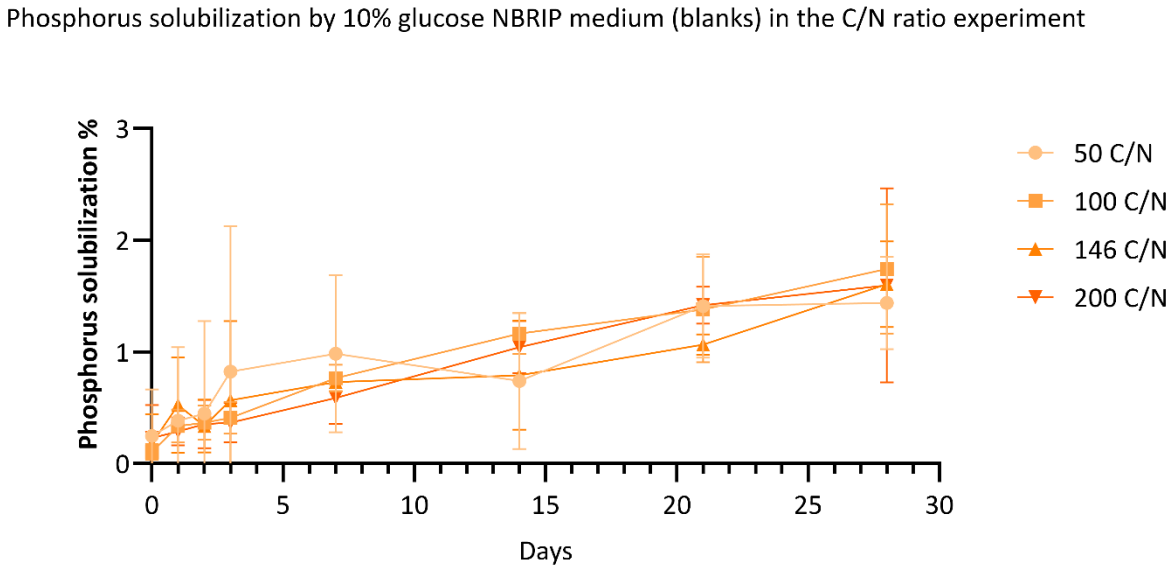

Figure A2. Phosphorus solubilization 10% glucose NBRIP medium (blank) in the C/N ratio experiment. The 95% confidence interval of the average is shown with error bars (n=4).

APPENDIX 3. The initial experiment on day 14.

Figure A3. The initial experiment on day 14: The fungi had agglomerated in 3 out of 4 replicates.

APPENDIX 4. Problems with organic acid measurements.

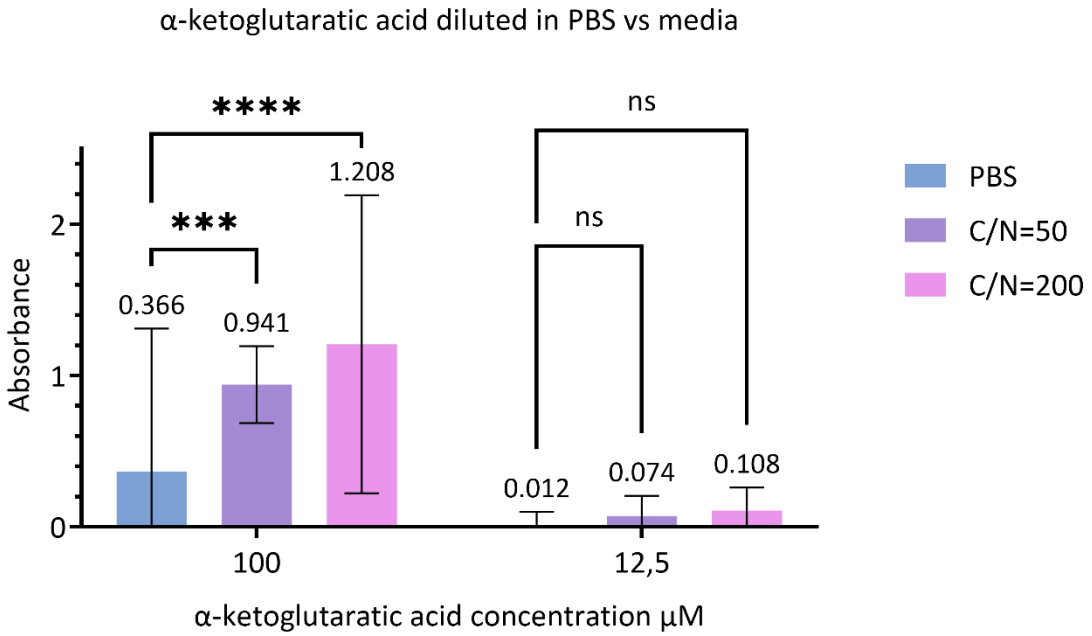

Figure A4. Absorbances of the α-ketoglutaric acid standard curve measurement. The graph shows the highest (100 µM) and the lowest (12,5 µM) α-ketoglutaric acid concentrations of the standard, after subtracting blank values. According to the protocol, standards must be diluted in PBS (phosphate-buffered saline). Too high absorbance of the standard diluted in the C/N=50 or C/N=200 NBRIP media shows working solution interaction with media. While at the lowest concentration the difference is non-significant, the highest concentration provides a significant difference between the use of PBS or media. The variance in measurements is shown with the 95% confidence intervals of the average (n=2). Statistical analysis was performed using two-way analysis of variance (ANOVA) followed by Tukey's post hoc test for multiple comparisons. Non-significant (ns) $p > 0.05$, * $p \leq 0.05$, ** $p \leq 0.01$, *** $p \leq 0.001$, **** $p \leq 0.0001$.

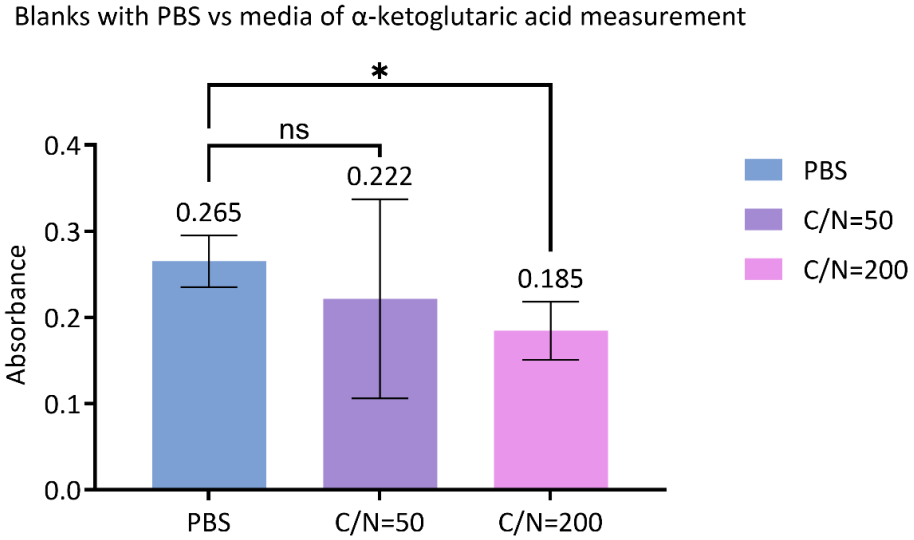

Figure A5. Absorbances of the blanks of the α-ketoglutaric acid measurement. According to the protocol, PBS (phosphate-buffered saline) is used in blanks. While the C/N=50 medium and PBS blanks have similar results, the PBS and C/N=200 medium are statistically significantly different. The variance in measurements is shown with the 95% confidence intervals of the average (n=3). Statistical analysis was performed using one-way analysis of variance (ANOVA) followed by Tukey's post hoc test for multiple comparisons. Non-significant (ns) $p > 0.05$, * $p \leq 0.05$, ** $p \leq 0.01$, *** $p \leq 0.001$, **** $p \leq 0.0001$.

APPENDIX 4. continues

Table A3. Absorbances of the standard curve of citric acid. A - absorbance. A1 - absorbance before colorimetric reaction. A2 - absorbance after colorimetric reaction. Values are presented after subtracting blank.

Standard concentration	A of the standard curve of citric acid	
g/L	A1	A2
0,2	-0,016	-0,381
0,1	0,028	-0,111
0,05	0,024	-0,065
0,01	0,025	-0,014
0,005	0,026	-0,039

Table A4. Citric acid absorbance measurements from 14-day samples. A - absorbance. A1 - absorbance before colorimetric reaction. A2 - absorbance after colorimetric reaction. Values are presented after subtracting blank. A2 values are in the range, however, the results can not be trusted due to A1 being too high compared to standards.

NBRIP media	A of 14-day sample	
	A1	A2
100 C/N	0,105	0,129
146 C/N	0,054	-0,028
200 C/N	0,047	-0,084

Too high A

Table A5. Absorbances of the standard curve of D-gluconic acid. A - absorbance. A1 - absorbance before colorimetric reaction. A2 - absorbance after colorimetric reaction. Values are presented after subtracting blank.

Standard concentration	A of the standard curve of the D-gluconic acid	
g/L	A1	A2
0,25	0,001	0,240
0,125	-0,019	0,137
0,05	0,013	0,042
0,01	0,032	0,016

Table A6. D-gluconic acid absorbance measurements from 28-day samples. A - absorbance. A1 - absorbance before colorimetric reaction. A2 - absorbance after colorimetric reaction. Values are presented after subtracting blank. A2 values are in the range, however, the results can not be trusted due to A1 being too high compared to standards.

NBRIP media	A of 28-day sample	
	A1	A2
100 C/N	0,091	0,061
146 C/N	0,072	0,058
200 C/N	0,064	0,063

Too high A

APPENDIX 4. continues

Table A7. Absorbances of the standard curve of tartaric acid. A- absorbance. A1 - absorbance before colorimetric reaction. A2 - absorbance after colorimetric reaction. Values are presented after subtracting blank.

Standard concentration	A of the standard curve of the tartaric acid	
g/L	A1	A2
5	-0,004	0,496
2,5	0,001	0,231
1,25	0,010	0,167
0,5	-0,003	0,051

Table A8. Tartaric acid absorbance 1 measurement from 28-day sample. A- absorbance. A1 - absorbance before colorimetric reaction. Values are presented after subtracting blank. A1 is too high compared to the standards.

Sample V, µl	A1 of 28-day sample		
	100 C/N	146 C/N	200 C/N
10	0,008	-0,025	-0,024
92	0,014	0,006	-0,004
185	0,047	0,025	0,014

Too high A

Table A9. Tartaric acid absorbance 1 measurement from 28-day sample. A- absorbance. A2 - absorbance after colorimetric reaction. Values are presented after subtracting blank. A2 values are under the range of the calibration curve.

Sample V, µl	A2 of 28-day sample		
	100 C/N	146 C/N	200 C/N
10	0,011	0,004	-0,005
92	0,014	-0,027	-0,016
185	0,041	-0,089	-0,021

Under calibration curve range

Non-exclusive licence to reproduce the thesis and make the thesis public

I, Keity-Carol Topper,

1. grant the University of Tartu a free permit (non-exclusive licence) to reproduce, for the purpose of preservation, including for adding to the DSpace digital archives until the expiry of the term of copyright, my thesis „**Bioleaching of phosphorus and rare earth elements (REEs) from Estonian phosphorite using *Aspergillus japonicus***“, supervised by Gintare Liudžiute and Priit Jõers.

2. I grant the University of Tartu a permit to make the thesis specified in point 1 available to the public via the web environment of the University of Tartu, including via the DSpace digital archives, under the Creative Commons licence CC BY NC ND 4.0, which allows, by giving appropriate credit to the author, to reproduce, distribute the work and communicate it to the public, and prohibits the creation of derivative works and any commercial use of the work until the expiry of the term of copyright.

3. I am aware of the fact that the author retains the rights specified in points 1 and 2.

4. I confirm that granting the non-exclusive licence does not infringe other persons' intellectual property rights or rights arising from the personal data protection legislation.

Keity-Carol Topper

25.05.2025